Research Square

Preprints are preliminary reports that have not undergone peer review.
They should not be considered conclusive, used to inform clinical practice,
or referenced by the media as validated information.

Assessment of Groundwater Potential Zone in Selamber District Using Integrated Geophysical, Remote Sensing, and Gis Techniques, Southern Ethiopia

Tekle Bangu
Arba Minch University
Arefegn Arota
Arba Minch University
Teklehaimanot Teklearegay
Arba Minch University
Tariku Degife
tarikudegife2015@gmail.com
Arba Minch University
Muralitharan Jothimani
Arba Minch University

Research Article

Keywords: Groundwater potential, remote sensing and GIS, Thematic map, VES

Posted Date: August 5th, 2026

DOI: https://doi.org/10.21203/rs.3.rs-10471674/v1

License: This work is licensed under a Creative Commons Attribution 4.0 International License.
Read Full License

Additional Declarations: No competing interests reported.

ASSESSMENT OF GROUNDWATER POTENTIAL ZONE IN SELAMBER DISTRICT USING INTEGRATED GEOPHYSICAL, REMOTE SENSING, AND GIS TECHNIQUES, SOUTHERN ETHIOPIA

Tekle Bangu[1*], Arefegn Arota[1*], Teklehaimanot Teklearegay[1*], Tariku Degife[1*], Muralitharan Jothimani[1*]

[1] *Department of Geology, College of Natural and Computational Sciences, Arba Minch University, Arba Minch, Ethiopia*

Corresponding Authors: Tariku Degife (tarikudegife2015@gmail.com),

Teklehaimanot Teklearegay (teklegeol23@gmail.com)

Abstract

Groundwater is one of the most valuable natural resources, an immensely important and dependable source of water supply for the rapidly growing population and urbanization in the given area. The majority of water used for domestic and agricultural purposes is obtained from groundwater sources rather than surface water, because surface water cannot meet the community's current water demand, especially during the dry seasons of the investigated area. Therefore, this study focused on assessing groundwater potential zones in the study area using integrated remote sensing, Geographic Information Systems (GIS), and Vertical Electric Sounding (VES) techniques. The thematic layers that were considered as control factors for groundwater occurrence in the study area are lithology, geomorphology, drainage density, lineament density, rainfall, soil, slope and land use/land cover were prepared from Landsat image using ArcGIS software. Weights were assigned to all these thematic layers according to their relative importance for groundwater occurrence, and the corresponding normalized weights were computed after hierarchical ranking using a pairwise comparison matrix of the Analytical Hierarchy Process (AHP). Finally, thematic layers were integrated in ArcGIS, and qualitative interpretation of the subsurface resistivity distribution was performed to produce a groundwater potential zone map. The developed groundwater potential zone map suggests that about 0.01%, 15.71%, 64.57%, 19.28%, and 0.43% of the groundwater potential were classified into very poor, poor, good, very good, and excellent categories, respectively. The main finding of this

investigation is the delineation of favorable sites for groundwater exploration and sustainable development, which helps decision-makers design an effective plan for the investigated area.

Keywords: Groundwater potential, remote sensing and GIS, Thematic map, VES

INTRODUCTION

Groundwater is the largest source of fresh water in the world. In many parts of the world, especially where surface water supplies are not available to meet domestic, agricultural, and industrial water needs, water beneath the ground can be used (Kumar, 1997). It is one of the key natural resources of the world. A number of cities and small towns worldwide depend on groundwater for water supplies because of its abundance, stable quality, and low cost to exploit, and particularly in areas with scarce surface water supplies (Morris *et al.,* 2003). The availability, accessibility, movement, and occurrence of groundwater depend on geology, slope aspect, lineaments, drainage density, land-use/land-cover, rainfall, surface runoff, and geomorphology of the area (Shaban *et al*., 2006). Evaluation, exploitation, exploration, site selection/delineation, and groundwater maps require serious attention, as they are cost- and time-effective; because they are outside our site, improper evaluation of groundwater and site selection are mostly expected to pose problems (Tesfaye, 2012).

Integrated approaches such as remote sensing, GIS, and geophysical (VES) methods have been key for studying the groundwater potential zone (Zaidi and Kassem 2012). Nowadays, these approaches have been advanced over time for groundwater investigation. Those approaches have played an important role in groundwater exploration for many years because of their reliability, ease of obtaining subsurface information, and non-destructive nature. The electrical resistivity survey using the Vertical Electrical Sounding (VES) method is the most popular geophysical technique for assessing groundwater potential (Ndatuwong and Yadav 2015).

The study area is located in the Southern Nation Nationalities and People's Regional State (SNNPR), Gamo Zone, Southern Ethiopia. In the investigated area, demand for clean water for drinking and other developmental activities is gradually increasing due to rapid population growth. However, there is insufficient amount of surface water especially in the dry seasons to address the current water demand for the society. Since most residents in the study area are rural people whose livelihoods are mainly dependent on agriculture, with poor water supply and sanitation services. Therefore, the exploration of groundwater resources can be considered the only viable means to balance water supply and demand and satisfy the community's largely livelihood needs without depleting the groundwater resource. This study aims to investigate the depth, thickness, and distribution of water-bearing formations and, finally, to delineate

groundwater potential zones using integrated VES, remote sensing, and GIS methods to address water scarcity problems in the study area.

Location of study area

The study area is located in the Southern Nations, Nationalities and Peoples' Region of Ethiopia within the Gamo zone. It is situated 235 km from the regional city named Hawassa, particularly, in the Southwest direction which is accessed through Hawassa -Wolaita Sodo -Selamber road and 395 km far away from Addis Ababa through the Addis Ababa–Wolaita Sodo– Gofa Sawula main road. The area is accessible by driving along a rough, dry-weather road and by foot paths that connect different parts of the study area. More specifically, the study area is bounded by a geographic coordinate system of Universal Transverse Mercator (UTM) zone 37N, between 37023'14" and 37045'18" easting and 6017'32" and 6^{0}38'35" northing (Fig.1).

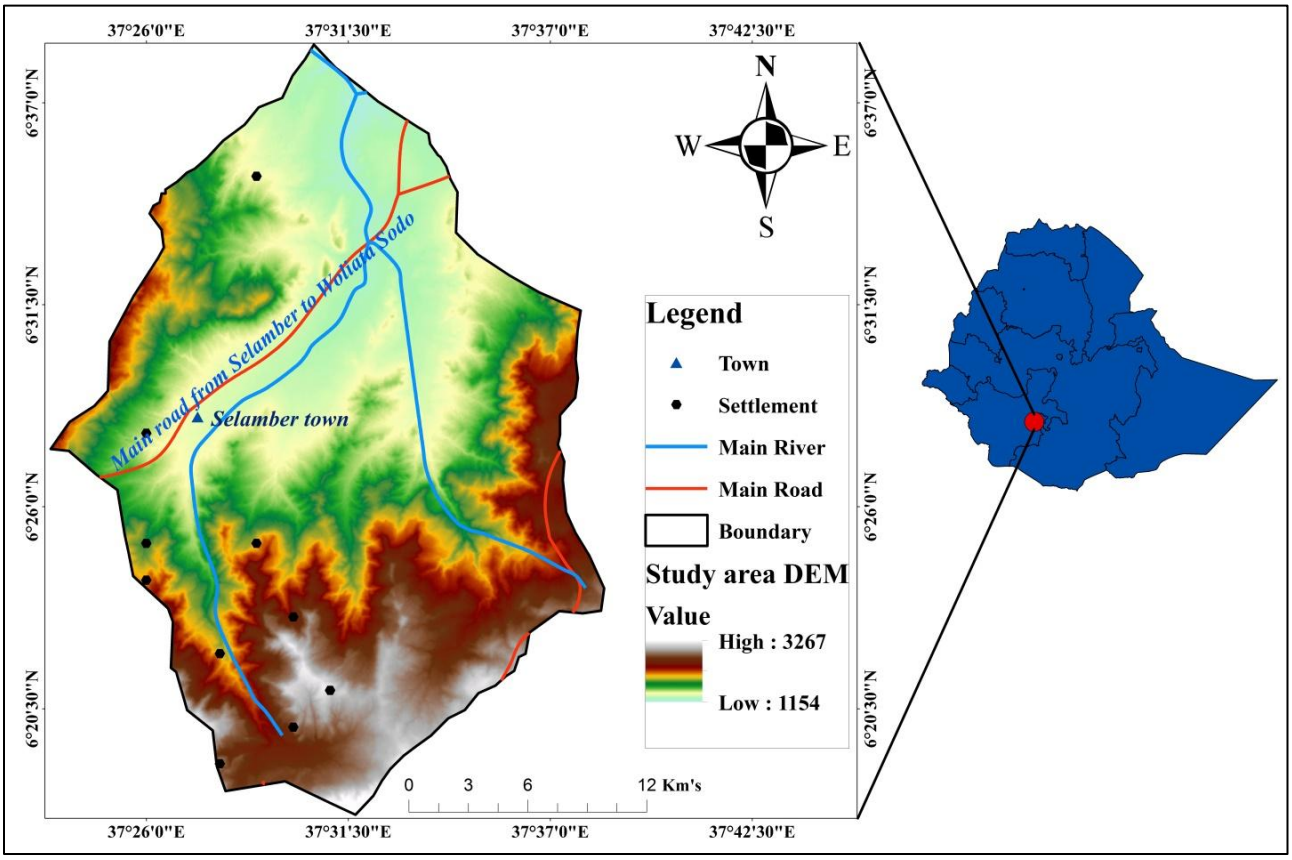


Fig.1: Location and accessibility map of the study area

Materials and methodology

To accomplish the objectives of the study, the following materials were used during fieldwork: Geophysical instrument (Resistivity), Topographic maps at scale 1:50,000, GPS, Digital Camera, and Compass.

Primary data collection was conducted through fieldwork to describe the lithology and geological structures, measuring their orientations, as well as to collect geophysical or resistivity data at selected stations in the study area using a systematic geo-traverse. Electrical Resistivity Vertical Electrical Sounding is a technique used to examine vertical changes in the resistivity of geological strata. The VES method employed by the company was carried out using a Schlumberger configuration. In this technique, the spacing between electrodes is progressively increased between measurements, while the array's center remains constant. As the electrode spacing increases, the current penetrates deeper. So, a plot of apparent resistivity versus electrode spacing provides a picture of resistivity variation with depth. The materials that have been used during the survey are a DDC-8 resistivity meter, 2 current electrodes (used to connect the ground), 2 potential electrode cables (used to push the current), a hammer (used to hit metal stakes), a GPS (which is used to take the geographic coordinates of the earth) and meter to measure the distance between two successive stations. The primary data collected during fieldwork and the available secondary data were processed and interpreted using various software packages, including Surfer, Win Resist, and IP2win, and existing borehole log data was used to confirm the results.

Generation of Geospatial Datasets

Both Remote Sensing and GIS approaches are essential tools for facilitating the integration and analysis of large volumes of data. Integration of the two technologies has proven to be an efficient tool for the exploration of the groundwater potential zone of a given area (Krishnamurthy et al., 1996). In this study, it was used to make digital image processing for the extraction of lithological and linear features, drainage density, LULC, slope and digital elevation model (DEM). DEM of 30 m resolution was downloaded from the SRTM website and used to extract lineament density, slope, drainage density, and topographic features of the study area. All data were integrated into a Geographic Information System (GIS) and analysed to evaluate the controlling factors of groundwater occurrence in the study area. Finally, a groundwater potential map was prepared based on the VES, remote sensing and GIS data analysis.

Analytic Hierarchy Process (AHP)

The AHP facilitates decision-making by organizing perceptions and judgments into a multi-level hierarchical structure that accounts for the forces that control a decision by assessing multiple factors (Yen et al., 2008). This method allows considering each of several properties separately for selecting the groundwater potential zone from competing sets of parameters. The method is implemented in four steps to delineate groundwater potential zones in the study area: (1) selecting factors that influence groundwater potential zones, (2) developing a pairwise comparison matrix, (3) estimating relative weights, and (4) assessing matrix consistency. Once the weights are assigned, it is required to calculate the consistency of the matrix; the consistency ratio is judged by the following equation:

$$\mathrm{CR} = \frac{CI}{RI} \quad (1)$$

Where; *CR* is the consistency ratio, *CI* is the consistency index, and *RI* is the random index

CI is calculated using the following equation:

$$\mathrm{CI} = \frac{\lambda\mathrm{max}-\mathrm{n}}{n-1} \quad (2)$$

Where; $\lambda\mathrm{max}$ is the principal eigenvalue of the matrix, and n is the number of factors considered for the groundwater potential.

Then, all the factors are classified into sub-classes and ranked by their impact on groundwater activities. Finally, the ranks of each sub-class were normalized by dividing each rank value by the sum of all ranks.

Table 1: Description of scales for pairwise comparison with AHP (Source: Saaty 1980)

Scales	Degree of preferences	Descriptions
1	Equal importance	• The contribution of the two factors is equally important
2	Equal to moderate importance	• Used to represent compromises between the preferences in weights 1 and 3
3	Moderate importance	• Experiences and judgment slightly tend to a certain factor
4	Moderate to strong importance	• Used to represent compromises between the preferences in weights 3 and 5

5	Strong importance	• Experiences and judgment strongly tend to a certain factor
6	Strong to very strong importance	• Used to represent compromises between the preferences in weights 5 and 7
7	Very strong importance	• A criterion is strongly favored over another, and its dominance is shown in practice
8	Very to extremely strong importance	• Used to represent compromises between the preferences in weights 7and 9
9	Extremely importance	• The evidence of favoring one criterion over another is of the highest degree possible of an affirmation

Table 2: Saaty's ratio index (RI) for different values of N

The consistency indices of randomly generated reciprocal matrices										
Order of matrix										
N	2	3	4	5	6	7	8	9	10	11
RI	0.00	0.52	0.90	1.12	1.24	1.32	1.41	1.48	1.49	1.51

Where N: number of criteria used and RI: Random index

Validation of Groundwater Potential Zone

There are several methods for checking the accuracy and validation of groundwater potential maps generated by AHP. The most usable validation techniques that would be used for this study are existing well yield and lithological log data.

RESULTS

Analytical Hierarchy Process (AHP) and Weights Assignments for Thematic Layers

The analytic hierarchy process (AHP) developed by Saaty (1980) is used in this study as a decision-aiding method to finalize the weights assigned to different themes and their respective features used to decipher the groundwater potential zone. AHP is a simple, matrix-based technique that allows users to assess the relative weights of multiple criteria intuitively. It allows efficient group decision-making, where group members can use their experience, values, and knowledge to break a problem down into a hierarchy and solve it using AHP steps. It also incorporates systematic checks on the consistency of judgments, which is one of its strongest points compared to other multi-attribute value processes.

Deriving the weights using Analytic Hierarchy Process (AHP)

The weights of each factor were computed mathematically using the Analytic Hierarchy Process (AHP), followed by an expert-knowledge-driven method for assigning ranks to each layer and its sub-classes. The interrelationship among factors classes and assigning of ranks to factor's sub-classes was established based on author's expertise as well as a literature review. The methodology for deriving the weights to the thematic layers and their corresponding classes involves three steps viz. Construction of a pairwise comparison matrix, computation of the criterion weight/ priority vector, and estimation of the consistency ratio.

Table 3: Pairwise comparison matrix of the thematic layers

Factor	LT	LD	RF	SL	DD	LULC	Soil
LT	1	2	3	5	6	7	8
LD	0.5	1	2	3	5	6	7
RF	0.33	0.50	1	2	3	5	6
SL	0.20	0.33	0.50	1	2	3	5
DD	0.16	0.20	0.33	0.50	1	2	3
LULC	0.14	0.16	0.20	0.33	0.50	1	2
Soil	0.12	0.14	0.16	0.20	0.33	0.50	1
Sum	2.45	4.33	7.19	12.03	17.83	24.5	32

Where LT-Lithology, LD-Lineament Density, RF-Rainfall, SL-Slope, DD-Drainage Density, LULC-Land Use/Land Cover

Table 4: Normalized pairwise comparison matrix and weights of each factor

Factor	LT	LD	RF	SL	DD	LULC	Soil	GM	NW	W%	Sum PCM	λ_{max}
LT	0.41	0.46	0.42	0.42	0.34	0.29	0.25	2.58	0.37	37.00	2.45	0.90
LD	0.20	0.23	0.28	0.25	0.28	0.24	0.22	1.71	0.24	24.00	4.33	1.06
RF	0.13	0.12	0.14	0.17	0.17	0.20	0.19	1.12	0.16	16.00	7.19	1.15
SL	0.08	0.08	0.07	0.08	0.11	0.12	0.16	0.70	0.10	10.00	12.03	1.21
DD	0.07	0.05	0.05	0.04	0.06	0.08	0.09	0.43	0.06	6.00	17.83	1.10
LULC	0.06	0.04	0.03	0.03	0.03	0.04	0.06	0.28	0.04	4.00	24.50	0.98
Soil	0.05	0.03	0.02	0.02	0.02	0.02	0.03	0.19	0.03	3.00	32.00	0.87
Sum	1	1	1	1	1	1	1			100		7.26

Where, GM -Geometric Mean, NW- Normalised Weight, W%- Per cent Weight, PCM- Pairwise Comparison Matrix, λ_{max} -Vector Value

Analysis of Each Thematic Layer for Groundwater Prospect

a) Lithology

The occurrence of groundwater in the given area is influenced by the features of various water-bearing geological formations (Jana A., et al 2012). Groundwater occurrence in hard rock is moderate to high because it depends on the intensity of primary and secondary porosity, such as vesicles, fractures, lineaments, faults, and the like (Seenipandi et al., 2019). For groundwater recharge, more weathered, less dense, and more prone to fracturing rocks provide better infiltration and better control of runoff (Krishnamurthy et al., 2000).

The investigated area is dominantly covered by two groups of formations: the Jima volcanic series and the Nazret series. About 410.37 km2 (64.6%), 167.8 km2 (26.42%), and 57.03 km2 (8.98%) of the study region is covered by basalt, ignimbrite, and volcanic tuff, respectively. Though basalt covers a large part of the study area rather than the other two units, it is well fractured. Therefore, high weight is assigned to basalt. The units have been classified into three categories based on their suitability for groundwater occurrence. The AHP method was applied to derive the consistency ratios of the lithologic units using the weight-assigning technique described above in the methodology section. The pairwise comparison matrix and normalized

weights of the lithology features are shown in Table 5. The Consistency Ratio for lithologic units is 0.05, which is less than 0.1 (Table 6). So, this matrix is coherent or fit the requirement.

Table 5: Pairwise comparison matrix, normalized & final weight, and Eigen vector of lithology

Criteria	A	B	C	NW	Final Weight	λ_{max}
A	1	3	5	0.64	0.23	0.96
B	0.3	1	3	0.26	0.09	1.10
C	0.2	0.3	1	0.10	0.03	0.94
Sum	1.5	4.3	9	-	-	3.00

Where A=Basalt, B= Volcanic tuff, C= Ignimbrite

To find the final weights of each thematic layer, the normalized weights of table 4 were multiplied by the individual normalized weight of the subclass feature of each thematic layer.

Table 6: Area coverage for sub-classes and Consistency ratio of the lithology

Factor	Classes	Area in (Km^2)	Area in (%)	Groundwater prospect	CI	RI	CR
Lithology	Basalt	410.37	64.6	Very good	0	0.52	0
	Ignimbrite	167.8	26.42	Good			
	Volcanic tuff	57.03	8.98	Moderately good			

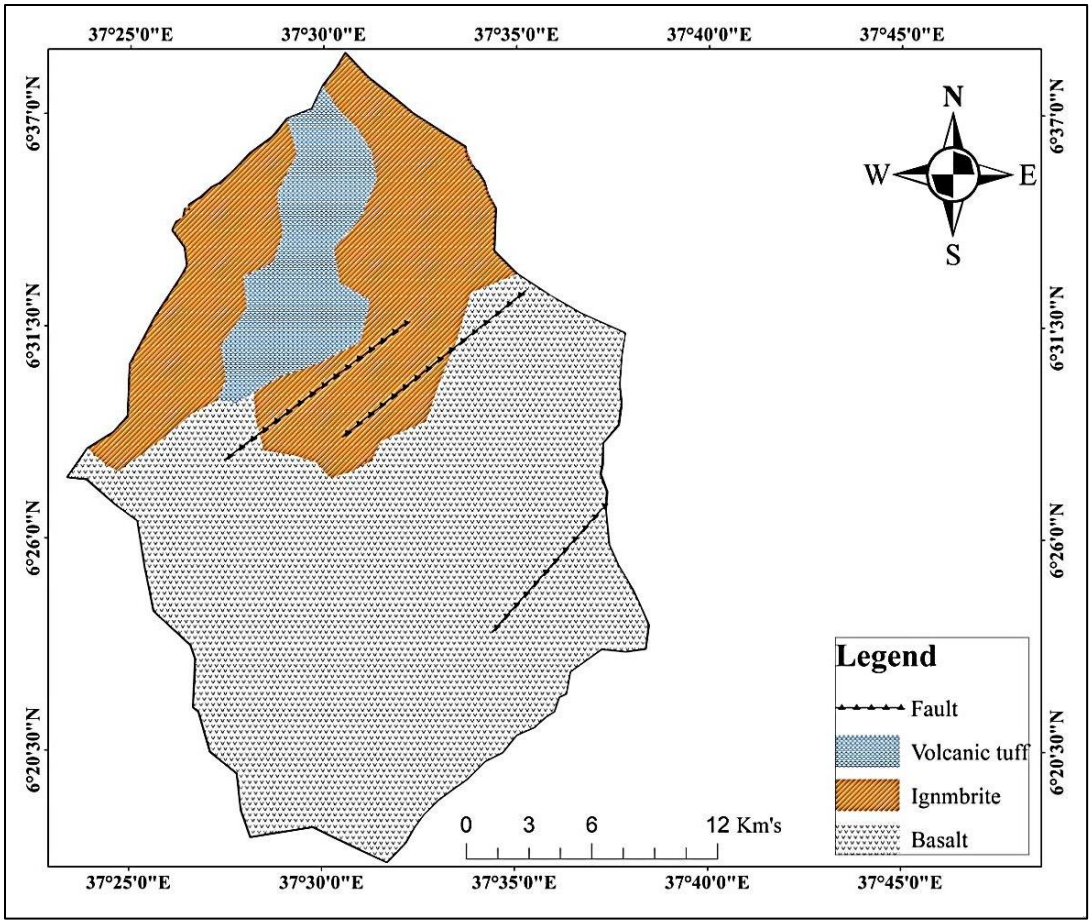


Fig.2. Geological map of the study area (Source: EGS, 2018)

b) Lineament Density

Lineaments are linear features of the Earth's crust that reflect subsurface geological structures, such as joints, cleavages, fractures, and faults, visible in satellite imagery. These weaker zones exhibit higher porosity and permeability, which are vital for groundwater potential (Goitsemang et al., 2020). Hence, it plays a significant role in the occurrence and movement of groundwater resources in crystalline rocks. Groundwater potential increases with increasing lineament density values (Varade et al., 2018). On the other hand, the intensity of groundwater potential decreases with increasing distance from the lineaments. Therefore, groundwater potential is high to very high in the region with high to very high lineament density (Lentswe & Molwalefhe, 2020).

In the study area, most lineaments are aligned with the drainage pattern trends (Fig.2). Additionally, structures such as faults, horsts and grabens are found in the study area. As shown above in the geological map (Fig.2), the orientations of faults follow the NE strike and dip

towards the NW because they are crucial for groundwater flow. Grabens are mostly found in the central parts of the investigated area, and other structures, such as joints, are observed in the basalt and ignimbrite units. Most of these geological structures' orientations follow the trend of EARS.

A lineament density map of the study area was prepared from the SRTM DEM at a resolution of 30m using ArcGIS 10.8 software. The created map has been reclassified as follows using the natural break method such as very low (0-0.019), Low (0.020-0.053), Low to moderate (0.054-0.081), Moderate (0.082-0.110), and High (0.120-0.180). The study area has very low lineament density, with the least aerial extent of high lineament density in the central and southwestern parts of the study area (Fig.2). It is also observed that high lineament density dominantly associated with basalt dominated regions, which could be due to deep faults or fractures in the area. More water movement occurs in areas with high lineament density due to their greater effective porosity and infiltration rates. Therefore, groundwater potential is tremendous in the region with moderate to high lineament density. Hence, high density is assigned a high weight, and low density is given a low weight.

The AHP method was adopted to derive the consistency ratio for lineament density using the weight-assigning technique described above in the methodology section. Its pairwise comparison matrix and normalized weights are shown in Table 7. The calculated Consistency Ratio of lineament density of the research area is 0.02, which is less than 0.1. Thus, the value fit the criteria in Table 6.

Table7: Pairwise comparison matrix, normalized and final weight, and Eigen value of lineament density

Criteria	A	B	C	D	E	NW	Final weight	λ_{max}
A	1.00	2.00	3.00	4.00	5.00	0.42	0.10	0.93
B	0.50	1.00	2.00	3.00	4.00	0.26	0.06	1.10
C	0.30	0.50	1.00	2.00	3.00	0.16	0.03	1.07
D	0.25	0.30	0.50	1.00	2.00	0.10	0.02	1.02
E	0.20	0.40	0.30	0.50	1.00	0.07	0.01	1.03
Sum	2.25	4.20	6.80	10.50	15.00			5.15

Where A= High (0.120-0.180), B= Moderate (0.082-0.110), C= Low to moderate (0.054-0.081), D= Low (0.020-0.053), E= Very low (0-0.019).

Table 8: Calculated area coverage for sub-classes and Consistency ratio of the lineament density

Factor	Classes (Km/Km^2)	Area in (Km^2)	Area in (%)	Groundwater prospect	CI	RI	CR
Lineament density	0.00-0.019	255.72	40	Very low	0.03	1.12	0.02
	0.020-0.053	128.82	20	Low			
	0.054-0.081	173.47	27	Low to moderate			
	0.082-0.110	51.27	8	Moderate			
	0.120-0.180	25.72	5	High			

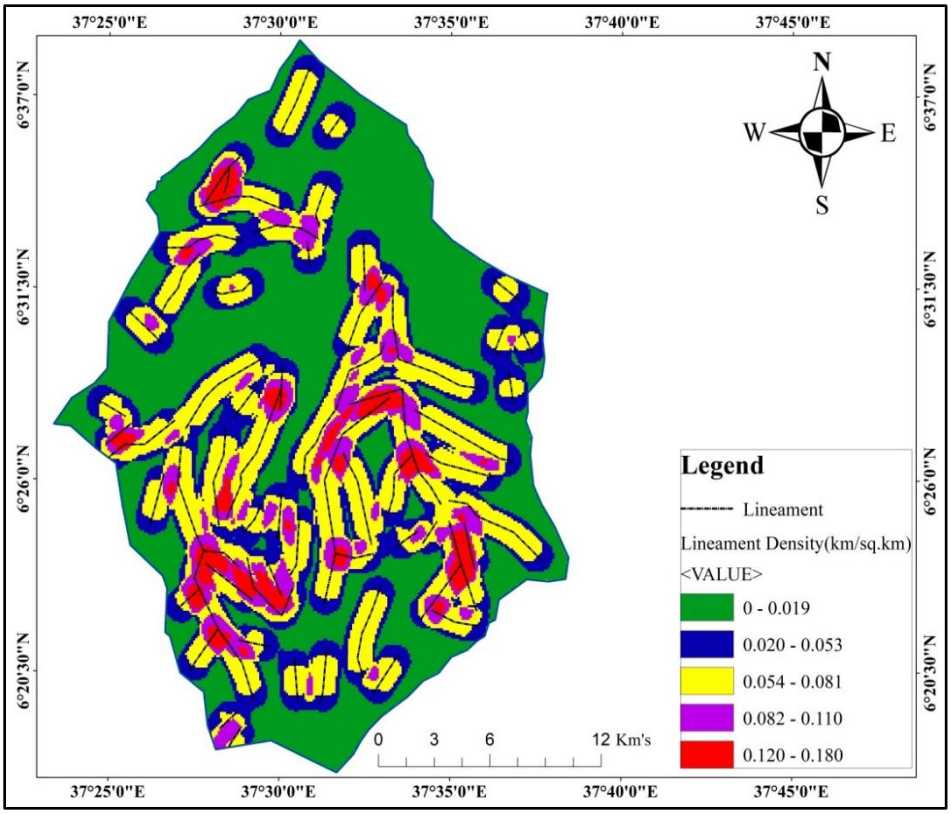


Fig.3. Lineament density of the study area

c) Rainfall

There is a direct correlation between the amount of rain that falls on a given area and the amount of groundwater that can be recharged into that area. High rainfall in a particular area increases the likelihood of groundwater recharge in that region, and vice versa (Machiwal et al., 2011). Therefore, to determine the amount of rainfall in the study area, about 18 years (2003-2021) of

data were collected from 32 stations using the online Climate Research Unit (CRU) data source. The rainfall map was prepared in ArcGIS software using the inverse distance weighted (IDW) interpolation technique. Thus, the results show that the average annual precipitation in the study region ranges from 297 to 1154 mm.

Based on its maximum and minimum mean values, rainfall has been reclassified into five categories using natural break, namely, Very low (297- 477 mm), Low (478- 624 mm), Low to moderate (625–756 mm), Moderate (757-890 mm) and High (891–1154 mm) (Jenks, 1967). The amount of rainfall is higher in the southern parts of the study area and decreases toward the northern parts, i.e., from highland to lowland (Fig.4). The AHP method was applied to derive the consistency ratio of the average annual rainfall using the formulas of weight assigning technique which is mentioned above in methodology section. The pairwise comparison matrix and normalized weights of the annual rainfall are shown in (Table 9). The calculated Consistency Ratio of average annual rainfall of the study area is 0.02, which is less than 0.1. Thus, the matrix met the criteria for a high degree of reliability (Table 10).

Table 9: Pairwise comparison matrix, Eigen value, normalized & final weight of rainfall

Criteria	A	B	C	D	E	NW	Final weight	λ_{max}
A	1.00	2.00	3.00	4.00	5.00	0.42	0.06	0.93
B	0.50	1.00	2.00	3.00	4.00	0.26	0.04	1.10
C	0.30	0.50	1.00	2.00	3.00	0.16	0.02	1.07
D	0.25	0.30	0.50	1.00	2.00	0.10	0.01	1.02
E	0.20	0.40	0.30	0.50	1.00	0.07	0.01	1.03
Sum	2.25	4.20	6.80	10.50	15.00			5.15

Where; A= Very low (297-477 mm), B= Low (478-624mm), C= Low to moderate (625–756 mm), D= Moderate (757-890 mm) E=High (891–1154 mm).

Table 10: Area coverage for each sub-classes and Consistency ratio of the rainfall

Factor	Classes (mm)	Area in (Km^2)	Area in (%)	Groundwater prospect	CI	RI	CR
Rainfall	297-477	82	13	Very low	0.03	1.12	0.02
	478-624	104.9	17	Low			
	625-756	171.6	27	Low to moderate			
	757-890	139.46	22	Moderate			

	891-1154	137.04	21	High			

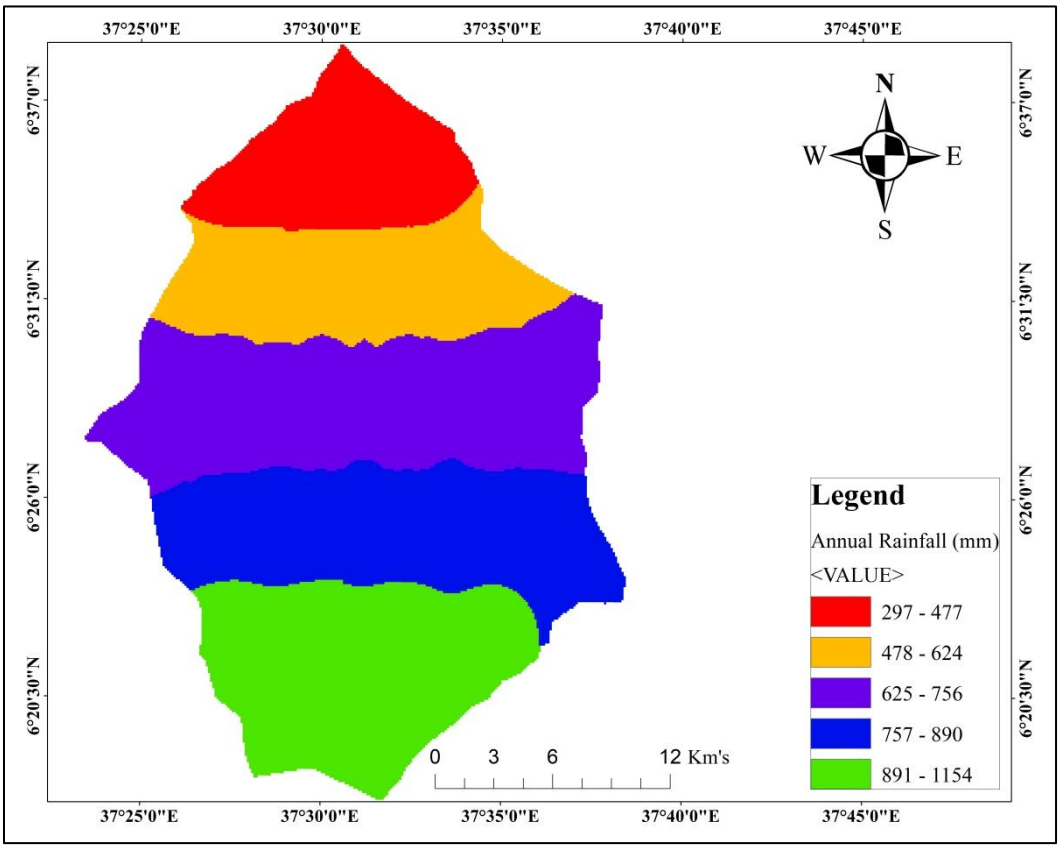


Fig.4. Rainfall map of the study area

d) Slope

The slope of a surface is the elevation change that determines the gravity influence on water movement (Manap et al., 2011). It regulates surface water infiltration into the subsurface, making it a good predictor of potential groundwater resources. In general, slope and infiltration rate are inversely proportional (Satapathy& Syed, 2015). The slope gradient affects the rate of water percolation and infiltration into the ground (Siva et al., 2017). Groundwater potential is found in areas with lower slope, while areas with higher slope are considered unsuitable (Shao et al., 2020). Therefore, the highest ratings were assigned to the low slope areas. The study area has been classified into five slope categories: flat (0 - 7°), gentle (7.1 - 14°), moderate (15 - 21°), steep (22 - 31°), and very steep (32 - 64 °). The AHP method was used to derive the consistency ratio for the slope using the weight-assignment technique. The analyzed pairwise comparison matrix and final normalized weights of each subclass were shown in Table 11. The calculated

Consistency Ratio for the slope of the research area is -0.001, which is less than 0.1. Therefore, the value fit the criteria (Table 12).

Table11: Pairwise comparison matrix, normalized& final weight, and Eigen value of slope

Criteria		A	B	C	D	E	NW	Final weight	λ_{max}
A		1	2	3	5	6	0.44	0.04	0.95
B		0.5	1	2	3	5	0.27	0.02	1.06
C		0.3	0.5	1	2	3	0.15	0.01	1.04
D		0.2	0.3	0.5	1	2	0.09	0.009	1.03
E		0.16	0.2	0.3	0.5	1	0.05	0.005	0.92
Sum		2.16	4	6.8	11.5	17			4.99

Where A= 0-7 (Flat), B=7.1-14 (Gentle), C=15-21 (Moderate), D=22-31 (Steep), E= 32-64(Very steep)

Table 12: Calculated areal coverage for subclasses and Consistency ratio of the slope

Factor	Classes (º)	Area in (Km^2)	Area in (%)	Groundwater prospect	CI	RI	CR
Slope	0-7 (Flat)	212.68	33	High	-0.002	1.12	-0.001
	7.1-14 (Gentle	183.91	29	Moderate			
	15-21 (Moderate)	118.65	19	Low to moderate			
	22-31 (Steep)	81.96	13	Low			
	32-64 (Very steep)	37.8	6	Very low			

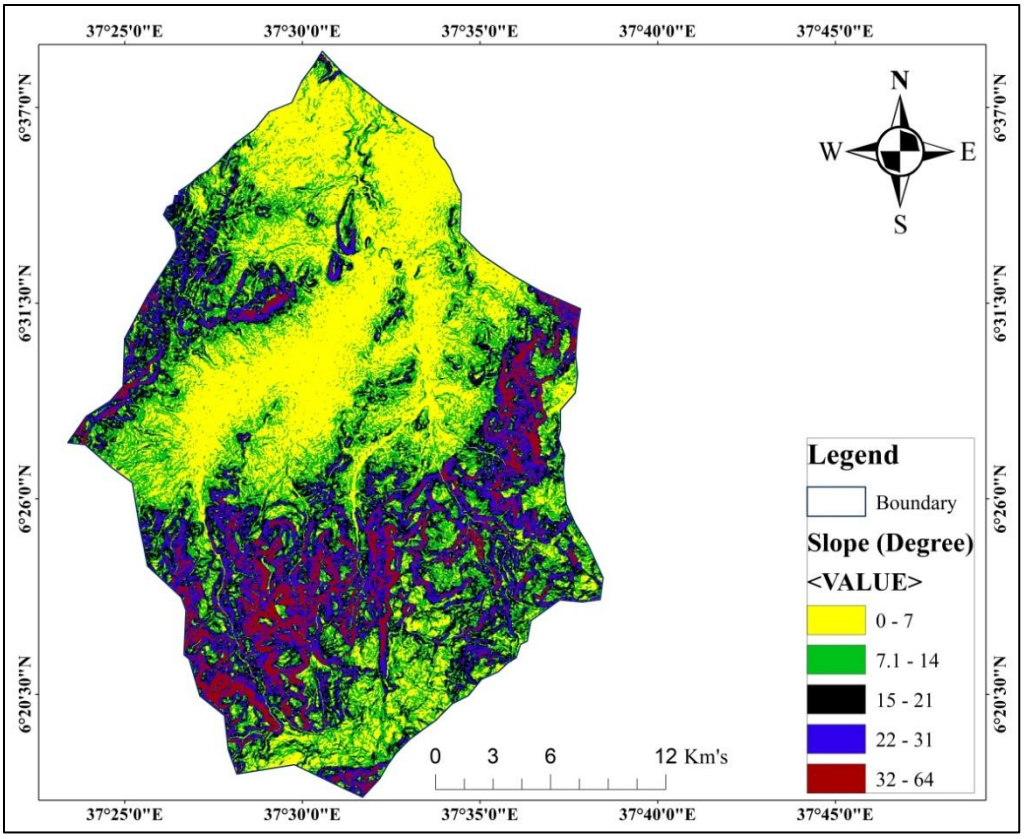


Fig.5. Slope map of the study area

e) Drainage Density

The rate of water flow and percolation into the aquifer are influenced by drainage density (Thapa et al. 2017). It is calculated by dividing the stream length by the drainage basin area. However, drainage density is influenced by lithology, which in turn determines infiltration rates (Abijith et al., 2020). Higher drainage density results in higher runoff, which reduces water infiltration into the subsurface (Bera et al., 2019). Regions with high drainage density have lower groundwater recharge, and vice versa (Halder et al. 2020). Thus, areas with low drainage density exhibit high groundwater potential (Mandal et al. 2016). Therefore, higher weights were assigned to the areas having low drainage density. A drainage density map of the research area was prepared from the SRTM DEM at a resolution of 30x30 using ArcGIS 10.8. According to Horton (1945), the created map has been reclassified and categorized as very low (0-0.83km/km^2), low (0.83-1.00 km/km^2), moderate (1.00-1.19km/km^2), and high (1.19-1.58km/km^2).

Based on the AHP technique, the consistency ratio for the drainage density was calculated using the weight-assigning scheme described in the methodology section. Its pairwise comparison

matrix and normalized weights are shown in table 13. The calculated Consistency Ratio of lineament density of the research area is -0.003, which is less than 0.1. Hence, the value fulfills the criteria as shown in Table 14.

Table 13: Pairwise comparison matrix, normalized weight, and Eigen value of drainage density

Criteria	A	B	C	D	NW	Final weight	λ_{max}
A	1	2	3	4	0.47	0.02	0.96
B	0.5	1	2	3	0.28	0.01	1.06
C	0.3	0.5	1	2	0.16	0.009	1.03
D	0.25	0.3	0.5	1	0.09	0.005	0.94
Sum	2.05	3.8	6.5	10			3.99

Where A= 0-0.83B= 0.83-1.00C= 1.00-1.19 D=1.19-1.58

Table 14: Calculated area coverage for sub-classes and Consistency ratio of the drainage density

Factor	Classes	Area in (Km^2)	Area in (%)	Groundwater prospect	CI	RI	CR
Drainage density	0.00-0.83	278.61	44%	High	-0.003	0.90	-0.003
	0.83-1.00	172.83	27%	Moderate			
	1.00-1.19	128	20%	Low			
	1.19-1.58	55.56	9%	Very low			

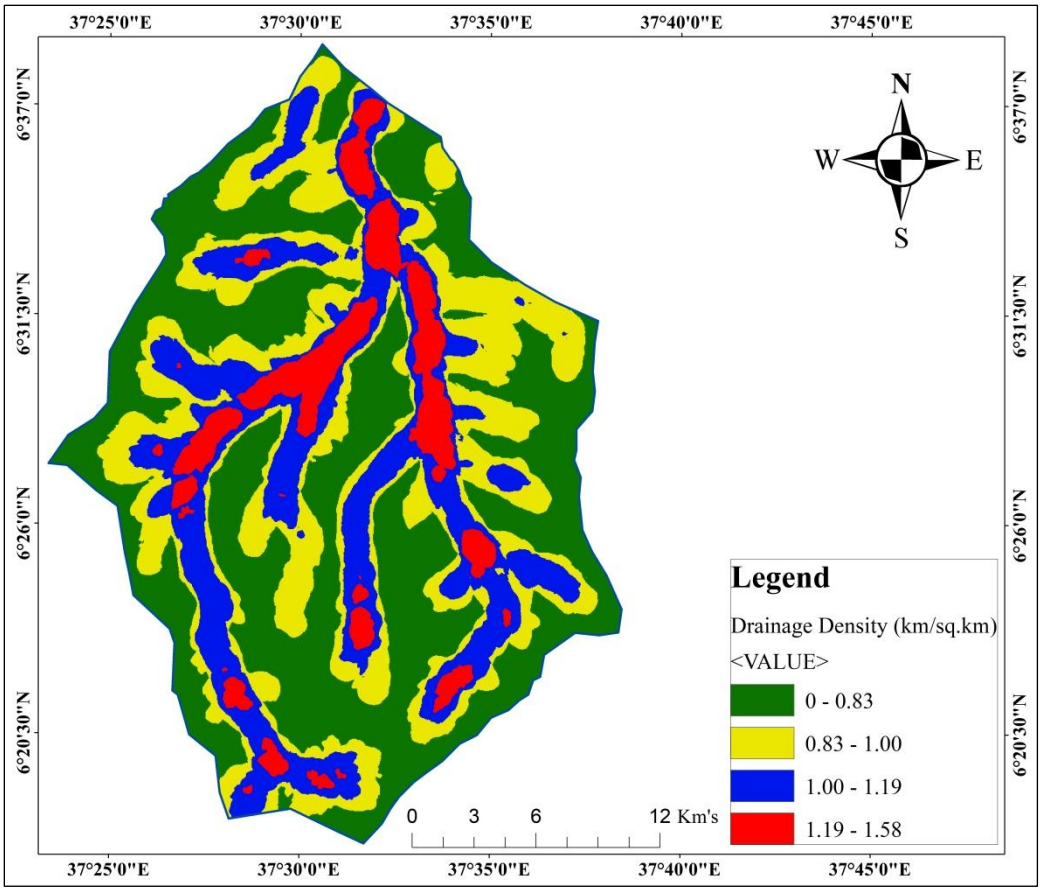


Fig.6. Drainage density map of the study area

f) Land Use and Land Cover

LULC provides vital details on soil moisture, infiltration, surface water, and other water resources, as well as indications of groundwater requirements. The LULC map indicates the extent of pavement areas, which are related to the availability of percolating water (Patil & Mohite, 2014). Groundwater depletion occurs in areas with wastelands and densely populated areas, while the water table rises in forest areas due to low runoff and high subsurface infiltration (Sahoo et al., 2017). Likewise, surfaces with dense vegetal cover have a greater capacity for infiltration than bare land. As a result, groundwater potential is exceptionally high in areas covered by forest and agricultural land (Li et al., 2018). The LULC map was prepared by downloading Landsat 8 images from the USGS Earth Explorer (https://earthexplorer.usgs.gov) website for the research area.

An image composite was created using the process toolbox from bands 1, 2, and 3, and the resulting image was extracted using the boundary of the study area with the help of the extraction tool in the spatial analysis tools. The LULC classification was done with the help of the training sample manager tool, which was used to select representative LULC classes, and the base map was used. This classification was supervised because training samples were used. The LULC map was constructed using a supervised maximum likelihood classification approach. The most likely image classification was then used to build the LULC map, which was categorized into five classes.

As shown in the figure below, about 33.07%, 28.666%, 20.7%, 16%, and 1.5% of the study area is covered by cultivated land, vegetation, built-up area, barren land, and water bodies, respectively. The study area is predominantly covered by built-up areas, which cover most of the western and northwestern parts and a few of the southern parts. Similarly, most of southern and central parts of the study area are covered by vegetation. As shown in the figure below, the lowland parts of the study area were dominated by barren land, and the remaining parts were occupied by water bodies and cultivated land (Fig.7).

The AHP method was adopted to derive the consistency ratio for lineament density using the weight-assigning technique described above in the methodology section. The calculated Consistency Ratio of lineament density of the research area is 0.02, which is less than 0.1. Thus, the value met the criteria (Table 16).

Table 15: Pairwise comparison matrix, normalized& final weight, and eigenvalue of LULC

Criteria	A	B	C	D	E	NW	Final weight	λ_{max}
A	1.00	2.00	3.00	4.00	5.00	0.42	0.016	0.93
B	0.50	1.00	2.00	3.00	4.00	0.26	0.010	1.10
C	0.30	0.50	1.00	2.00	3.00	0.16	0.006	1.07
D	0.25	0.30	0.50	1.00	2.00	0.10	0.004	1.02
E	0.20	0.40	0.30	0.50	1.00	0.07	0.002	1.03
Sum	2.25	4.20	6.80	10.50	15.00			5.15

Where A= Water body, B=Vegetation, C= Cultivated land D= Barren land, E= Built up area

Table 16: Calculated area coverage for sub-classes and Consistency ratio of the LULC

Factor	Classes	Area in (Km^2)	Area in (%)	Groundwater prospect	CI	RI	CR
LULC	Built up area	132	20.70	Very poor	0.03	1.12	0.02
	Barren land	101	16	Poor			
	Cultivated land	210	33.07	Moderately good			
	Vegetation	182	28.66	Good			
	Water body	10	1.57	Very good			

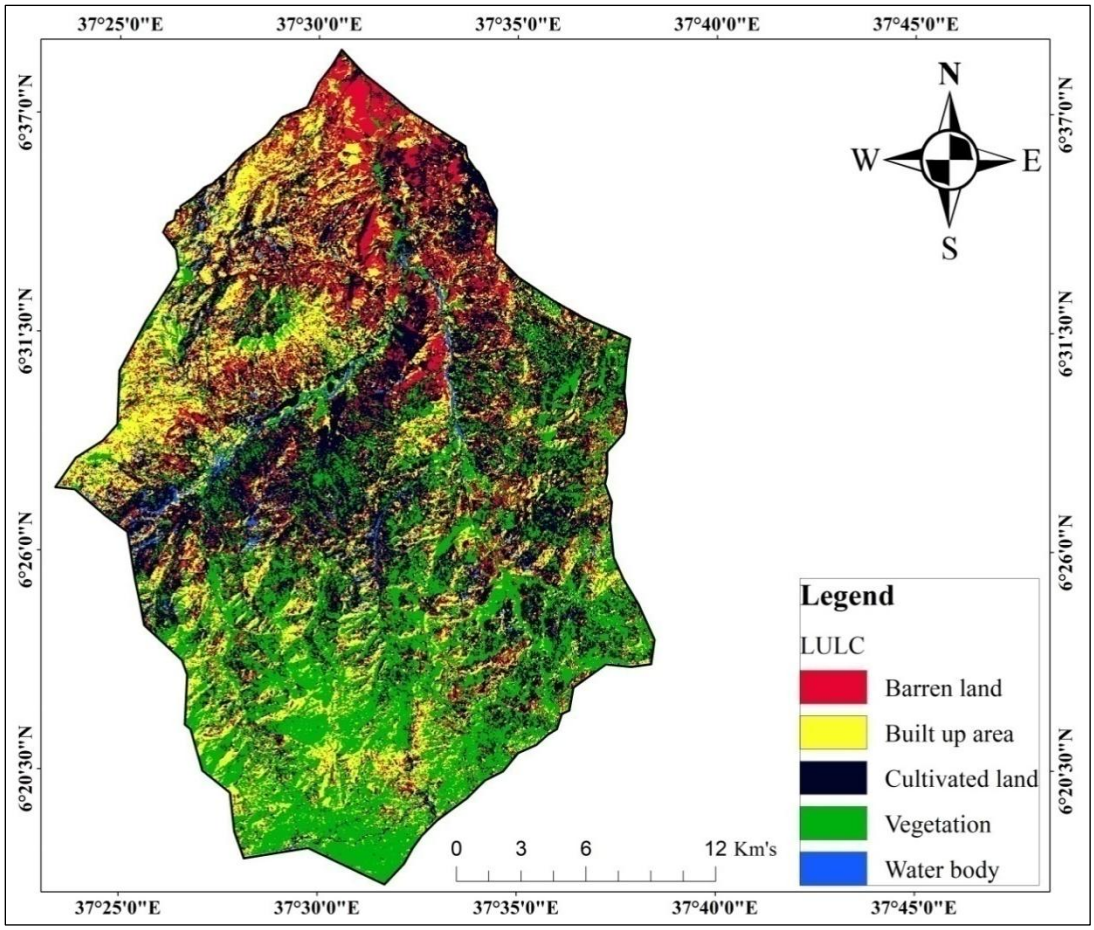


Fig.7. Land use/land cover map of the study area

g) Soil

Soil is one of the parameters that govern the percolation of surface water into the groundwater (Abijith et al., 2020). Its texture and hydraulic characteristics are the primary factors considered when estimating the infiltration rates. Generally, soil permeability, water retention capability, and soil type influence infiltration rates (Gupta et al., 2018). Based on the available GSE soil shape file and FAO (1985), soil classification, the study area is covered by orthic acrisols (223.8km^2), eutric cambisols (43.85km^2), dystric nitisols (316km^2) and dystric fluvisols (51.37km^2). When assigning weights for individual soil units, soil types and infiltration rates were considered.

Dystric fluvisols are genetically young soils in alluvial deposits deposited under natural conditions, which contain a low content of unstable grains such as feldspar and volcanic fragments (Agezew, 2015). Similarly, Eutric Cambisols are typically from volcanic as well as alluvial, colluvial, and aeolian deposits. In terms of texture, it is composed of clay-sized particles (GSE, 2014). Orthic Acrisols: this soil type is derived from tertiary volcanic rocks and basement rock and is used for various agricultural activities (Birhan et al., 2018). Dystric nitisols are mainly clay soils; most of the study area is covered by this soil type (Fig.8). Dystic nitisols also have a low content of unstable grains, such as feldspar and others (Agezew, 2015). The porosity and permeability of sandy loam are relatively higher than those of clay soil. Hence, the recharge capacity is also high in those soils. Thus, due to low clay content and high infiltration rate, dystric fluvisols were given the highest weight compared to the other soil types.

The AHP method was used to derive the consistency ratio of the soil using the weight-assigning technique. The analyzed pair wise comparison matrix and final normalized weights of each subclass were shown in Table 17. The calculated Consistency Ratio of the soil in the study region is -0.003, which is less than 0.1. Therefore, the value fits the criteria (Table 18).

Table 17: Pairwise comparison matrix, normalized & final weight, and Eigen value of soil

Criteria	A	B	C	D	NW	Final weight	λ_{max}
A	1	2	3	4	0.47	0.014	0.96
B	0.5	1	2	3	0.28	0.008	1.06
C	0.3	0.5	1	2	0.16	0.004	1.03
D	0.25	0.3	0.5	1	0.09	0.002	0.94

Sum	2.05	3.8	6.5	10			3.99

Where A=Dystricfluvisols, B= EutricCambisols, C= OrthicAcrisols, D=Dystricnitisols

To find the final weights of the soil, the normalized weights from table (4.2) were multiplied by the individual normalized weights of the soil.

Table 18: Calculated area coverage for sub classes and Consistency ratio of the soil

Factor	Classes	Area in (Km^2)	Area in (%)	Groundwater prospect	CI	RI	CR
Soil	Dystricfluvisols	51.37	8.10	High	-0.003	0.9	-0.003
	EutricCambisols	43.85	49.76	Moderate			
	OrthicAcrisols	223.78	6.90	Low			
	Dystricnitisols	316	35.24	Very low			

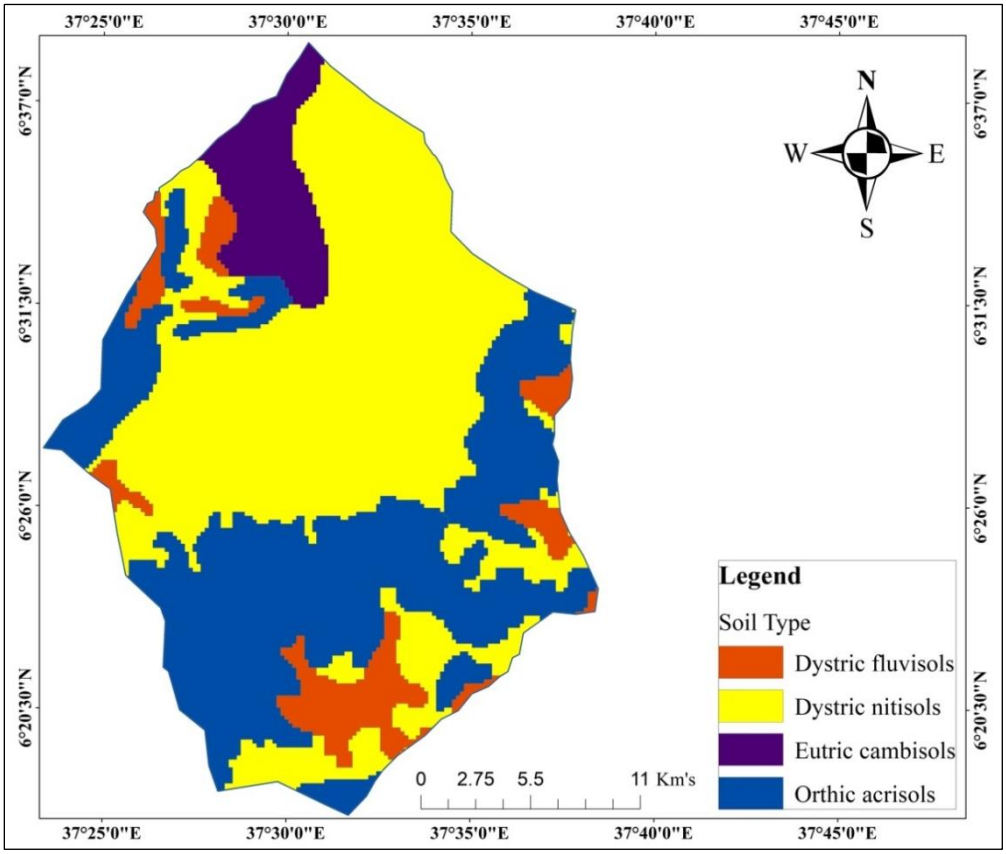


Fig.8. Distribution of soil types in the study area (Source: Shapefiles from GSE)

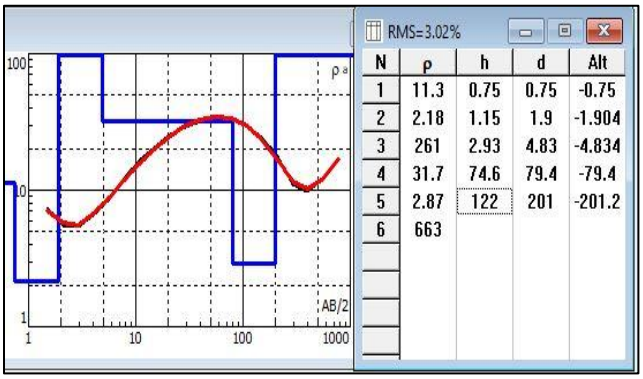
Resistivity Survey result

The interpretation of VES resistivity point data across all profiles is presented in this section. Generally, 5 VES (VES-1, VES-2, VES-3, VES-4, and VES-5) points were conducted within the project area. By observing the shape of the field curves (VES curves), a qualitative interpretation of the subsurface resistivity distribution can be performed. Thus, the vertical electrical sounding curve types identified in the investigated area include HKQH, HKHA, QHA, HAAK, and HAA. From these, the HKQH, HKHA, and HAAK-type curves represent the sixth-layer models, while the remaining curves represent the five-layer models (QHK & HKA). The HKQH-type curve implies that the intermediate layer has higher resistivity than the top and bottom layers. QH type curve denotes that hard rock overlain by soft strata, which can be good for groundwater potential zone (Gaikwadet al., 2021). The VES curves related with H-type indicating water potential sites. Whereas VES curves associated with A-type suggest hard rock terrain (Patil et al., 2020). HAK and HKH are the major curve types in the five layers. VES curves containing H or K types demonstrating good groundwater accumulation and storage (Gaikwad et al., 2021).

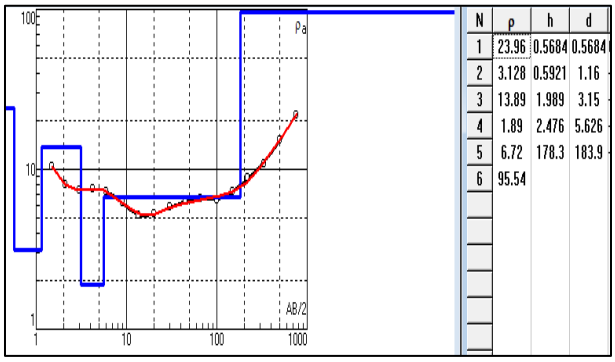
From the Fig.9 (A) VES-1 refers HKQH-type curve ($\rho_1 < \rho_2 > \rho_3 > \rho_4 > \rho_5 < \rho_6$). The first layer group, with a resistivity of 11.3 Ωm and a thickness of 0.75 m, is related to water-saturated volcanic ash, sand & tuff. The second layer, with a resistivity of 2.18 Ωm, is interpreted as weathered or fractured basalt intercalated with silt and sand, whereas the third layer, characterized by a resistivity of 261 Ωm, may be related to a fractured volcanic unit. The fourth layer, with a resistivity of 31.7 Ωm and a thickness of 2.93m, and the 122 m-thick fifth layer, with a resistivity of 2.87 Ωm, are the main water-bearing horizons. Finally, the sixth layer with a high resistivity (663 Ωm) below 201m depth is interpreted as fractured basalt. From Fig.9 (B): VES-2 implies an HKHA-type curve ($\rho_1 > \rho_2 < \rho_3 > \rho_4 < \rho_5 < \rho_6$) and the resistivity value of each layer is interpreted as clay soil intercalated with dry alluvial deposit/ water saturated highly weathered volcanic ash, sand & tuff. From Fig.9(C): VES-3 indicates QHK -type curve ($\rho_1 > \rho_2 > \rho_3 < \rho_4 < \rho_5$) and at this VES points the resistivity value signifies that the lithology of the area could be weathered or fractured basalt/alluvial deposit. From Fig.9 (D): VES-4 demonstrates HAKH curve types ($\rho_1 > \rho_2 < \rho_3 < \rho_4 > \rho_5 < \rho_6$) and VES-5 represented HKA.- type curve ($\rho_1 > \rho_2 < \rho_3 < \rho_4 < \rho_5$). Again, from both VES points, resistivity values are expected for water-saturated, highly weathered and fractured basalt, clay soil, volcanic ash, sand & tuff. In general, the resistivity values are do not vary significantly in all VES points which imply almost similar lithologies are found in the study

area. At all VES points, relatively low resistivity values have been identified at shallow depth, but some of them indicate that low-resistivity layers (especially below VES-4) are also found at depth. Thus, these are the sites where groundwater potential zone can be marked.

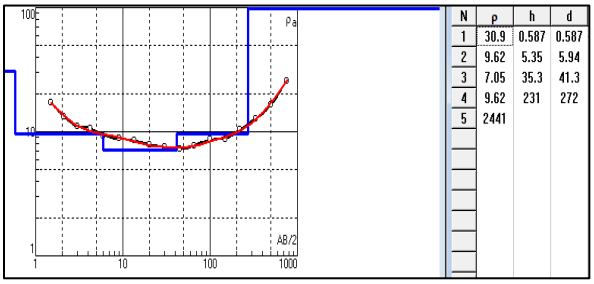
Two apparent resistivity pseudo-sections are plotted by using VES-1, VES-2, and VES-3 for pseudo section one which is oriented in the SW-NE direction, and VES-4, VES-2, and VES-5 for pseudo-section two in the NW-SE direction. Both apparent resistivity pseudo sections (Fig.10 and 11) indicate that low resistivity values were encountered by the layer which is found at shallow depth rather than the layer at great depth. This suggests that the shallow groundwater aquifer encountered in the study area.



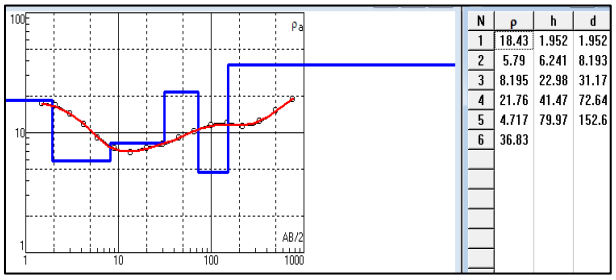
A. Geoelectric parameter of VES-1



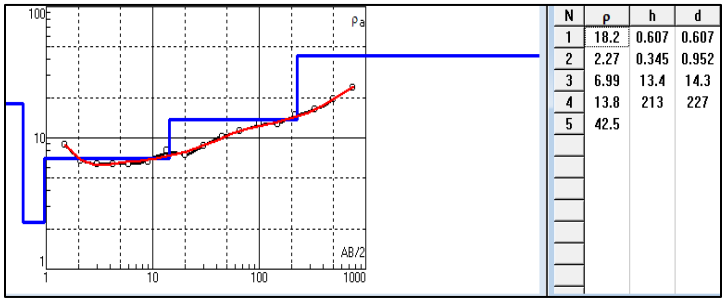
B. Geoelectric parameter of VES-2



C. Geoelectric parameter of VES-3



D. Geoelectric parameter of VES-4



E. Geoelectric parameter of VES-5

Fig.9: VES geoelectric curves

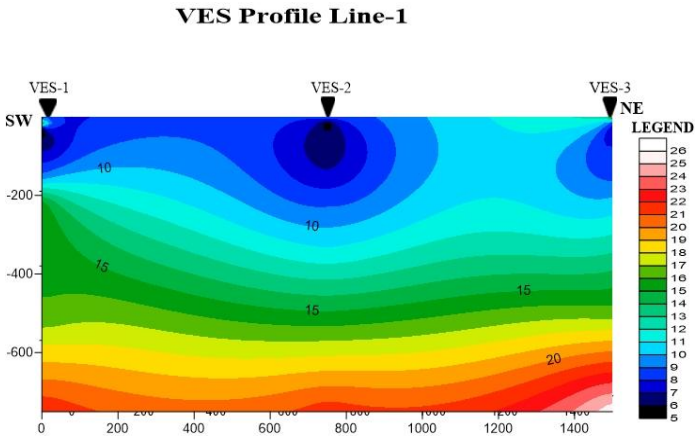


Fig.10. Apparent resistivity pseudo cross section for profile line one

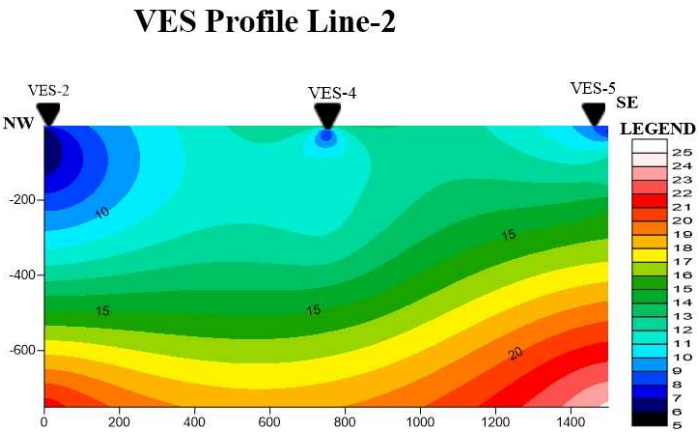


Fig.11. Apparent resistivity pseudo cross section for profile line two

Delineation of Groundwater Potential Zone

All the thematic maps were converted to raster format and superimposed using a weighted overlay analysis (rank-and-weight-wise thematic maps). The developed groundwater potential zone map within the study area reveals that about 0.01%, 15.71%, 64.57%, 19.28%, and 0.43% of the groundwater potential zone were classified into very poor, poor, good, very good, and excellent categories, respectively. It is derived from the integrated operation of various factors, including lithology, rainfall, lineament, drainage density, slope, LULC, and soil types. As shown

in (Fig.12) below, the excellent to very good potential zone has been detected in the southern, southeastern, central, and southwestern parts of the study area. In contrast, very poor to poor groundwater potential is located in the northern, northeastern, and northwestern parts of the study area.

Table19: Classification of Groundwater potential zone with their respective area coverage

Classification	Area	%
Very poor	0.09	0.01
Poor	99.75	15.71
Good	410.00	64.57
Very good	122.40	19.28
Excellent	2.76	0.43
Total	635.00	100.00

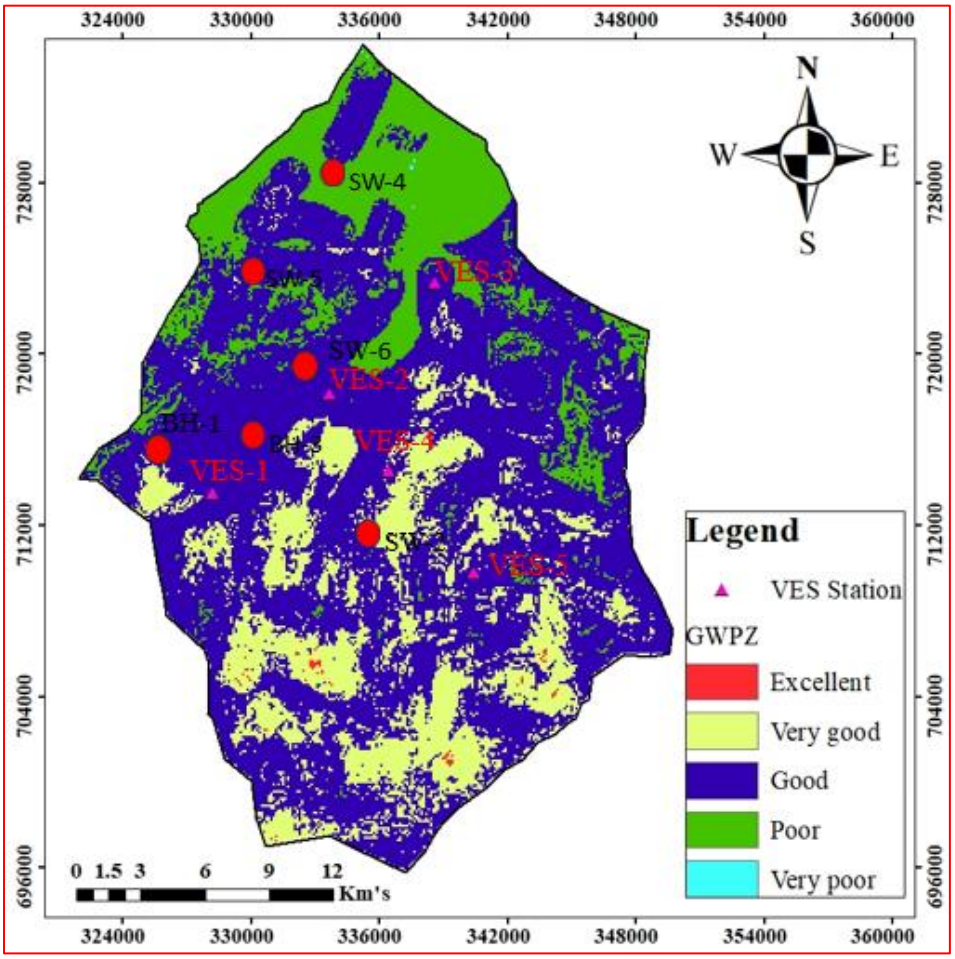


Fig.12. Groundwater potential zone map with VES station

Validation of the groundwater potential zone

In this study, the results have been validated using well yield data. The groundwater potential zones obtained by integrating RS, GIS, and VES were validated using data collected from five wells in the study area. Due to uneven distribution of well data, groundwater level map was not prepared. Thus, the validity of the groundwater potential map was assessed by overlaying point data from shallow and deep wells with the map generated using weighted index overlay analysis. Therefore, the actual yield data collected from the pumping test and the lithological log data indicate that the selected methodology implemented in this study is notably reliable and accurate.

Table 20: Well yield data

Wells	UTM coordinates		Elevation	TWD	Q (l/s)	Swl (m)	Dwl (m)
	Easting	Northing (m)					
BH-1	328964	715361	1377	77	3.25	25.2	54.3
Sw-2	335319	720641	1302	57	2.5	14.5	34.7
BH-3	329755	716504	1387	145	2.9	47.4	89
Sw-4	340565	725038	1282	53	1.2	13.1	30.3
Sw-5	332025	728498	1442	42	1.5	11.8	26.2
Sw-6	341759	712872	1711	59	2.2	22	35.1

Where TWD = total well depth, Q = well yield, Swl and Dwl = static and dynamic water level respectively (Source: South Design and Construction Supervision Enterprise)

Table 21: Lithological log data of borehole (BH-3) in the study region

Borehole (BH-3)	Coordinates	329455m E, 716504m N and at altitude of 1387m	
Layer	Depth (m)	Thickness (m)	Lithological description
1	0-4	4	Clay
2	4-8	4	Tuff
3	8-60	52	Volcanic ash, Sand, tuff
4	60-96	36	Weathered basalt
5	96-146	50	Fresh basalt

Discussions

The occurrence and distribution of groundwater in Selamber District are controlled by the complex interaction of geological, geomorphological, climatic, and hydrological factors rather than by any single parameter. In this study, the integration of remote sensing, GIS-based multi-criteria analysis, and Vertical Electrical Sounding (VES) provided a comprehensive approach for delineating groundwater potential zones. The generated groundwater potential map classified the study area into five categories, namely very poor (0.01%), poor (15.71%), good (64.57%), very good (19.28%), and excellent (0.43%) groundwater potential zones, respectively. The dominance of good and very good groundwater potential zones indicates that suitable hydrogeological conditions are widely distributed throughout the study area, whereas the limited extent of excellent potential zones represents locations where multiple favorable conditions such as suitable lithology, structural permeability, recharge availability, and terrain conditions occur together (Mohammed et al., 2025; Oyda et al., 2025; Tolba et al., 2026). The spatial distribution of groundwater potential zones reflects the combined influence of aquifer characteristics and recharge controlling factors (Das & Pardeshi, 2018; Khan et al., 2021; Rajaveni et al., 2017). Areas classified as very good and excellent potential zones are mainly associated with regions where geological structures, moderate to high lineament density, suitable rainfall conditions, gentle slopes, and favorable land cover characteristics occur simultaneously (Das & Pardeshi, 2018; Khan et al., 2021; Rajaveni et al., 2017). In contrast, poor and very poor potential zones are associated with areas where one or more controlling parameters restrict groundwater accumulation, such as unfavorable lithology, steep slopes, limited structural connectivity, or reduced infiltration capacity (Das & Pardeshi, 2018; Khan et al., 2021; Rajaveni et al., 2017).

Lithology represents one of the most important controlling factors for groundwater occurrence because it governs aquifer storage capacity, permeability, porosity development, and groundwater flow pathways. In the present investigation, lithology received the highest weight (37%) among all thematic layers, highlighting its dominant influence on groundwater potential assessment. The study area is mainly composed of basalt, ignimbrite, and volcanic tuff formations, with basalt covering approximately 64.6% of the total area. The relatively higher groundwater potential associated with basaltic formations can be explained by the development of secondary porosity caused by weathering, fracturing, vesicular structures, and tectonic deformation (Ayalew et al., 2019; Endyana et al., 2016; Fenta et al., 2020; Gastmans et al.,

2016). Although fresh basalt generally exhibits limited primary permeability, fractured and weathered basalt commonly forms productive aquifers because fractures provide pathways for infiltration and groundwater movement (Ayalew et al., 2019; Endyana et al., 2016; Fenta et al., 2020; Gastmans et al., 2016). The relatively lower groundwater suitability of ignimbrite and volcanic tuff units may be related to differences in permeability, degree of weathering, and fracture connectivity. Therefore, groundwater occurrence in volcanic terrains is strongly dependent not only on rock type but also on the intensity and distribution of secondary geological structures (Cid et al., 2021; Mihret & Wuletaw, 2025).

Lineaments and geological structures play a significant role in controlling groundwater movement and storage, particularly in hard-rock and volcanic environments. Lineaments represent zones of weakness associated with faults, fractures, joints, and other discontinuities that enhance secondary permeability and provide preferential pathways for groundwater migration (Oyda et al., 2025; Tolba et al., 2026). In the present study, areas with moderate to high lineament density showed better groundwater potential because fractured zones facilitate infiltration, recharge, and subsurface water movement. The association of high lineament density with basalt-dominated regions indicates that tectonic and structural processes have contributed significantly to groundwater development in the study area. The presence of faults, grabens, and fracture systems related to the East African Rift tectonic setting further supports the importance of structural controls on groundwater distribution (Ayenew et al., 2008; Bretzler et al., 2011; Kebede et al., 2008; Mechal et al., 2017). However, the hydraulic behaviour of faults depends on their orientation, fracture aperture, and infilling materials, as some faults may act as conduits while others may restrict groundwater flow (Anderson & Bakker, 2008; Sapkota et al., 2024).

Rainfall is another important factor influencing groundwater recharge because it determines the amount of water available for infiltration and aquifer replenishment. The rainfall analysis in the study area showed spatial variation from 297 to 1154 mm annually, with higher rainfall occurring mainly in southern highland regions. Areas receiving higher rainfall generally exhibited better groundwater potential because increased precipitation enhances recharge opportunities when favourable geological and geomorphological conditions exist (Moeck et al., 2020; Mohan et al., 2017). However, rainfall alone cannot determine groundwater availability because recharge efficiency depends on infiltration capacity, lithology, slope, drainage characteristics, and land surface conditions. Therefore, integrating rainfall information with other

controlling parameters provides a more realistic representation of groundwater potential (Fallatah et al., 2019; Ortenzi et al., 2026).

Slope conditions significantly influence groundwater recharge by controlling runoff velocity, infiltration time, and surface water retention. In general, gentle and flat terrain promotes infiltration by allowing longer contact time between surface water and soil, whereas steep slopes increase runoff and reduce infiltration opportunities (Oyda et al., 2025; Tolba et al., 2026). In Selamber District, areas with lower slope gradients were assigned higher groundwater suitability ratings because they provide favorable conditions for water infiltration and recharge. Similarly, drainage density influences groundwater occurrence by controlling runoff and infiltration behavior. Areas with high drainage density generally experience rapid runoff and limited infiltration, whereas low drainage density regions favour groundwater recharges due to increased infiltration potential (Jerin et al., 2025; Jothimani et al., 2022; Khanday & Javed, 2017). The observed relationship between slope, drainage density, and groundwater distribution confirms that surface morphology strongly regulates recharge processes in the study area.

Land use and land cover conditions also contribute significantly to groundwater recharge by influencing infiltration, evaporation, and surface runoff processes. Vegetated areas and agricultural lands generally enhance infiltration by reducing runoff velocity and improving soil moisture retention, whereas barren and highly disturbed surfaces may reduce recharge potential due to increased runoff (Oyda et al., 2025; Tolba et al., 2026). The incorporation of LULC as a thematic layer improved the groundwater potential model by representing the influence of surface conditions on aquifer replenishment. Similarly, soil characteristics influence groundwater availability by controlling infiltration rates and water retention capacity. Permeable soils facilitate downward movement of water, while compact or clay-rich soils restrict infiltration and reduce recharge potential (Oyda et al., 2025; Tolba et al., 2026).

The integration of VES data provided additional subsurface information and improved confidence in the groundwater potential assessment. The resistivity results helped identify variations in subsurface formations and possible water-bearing zones, supporting the interpretation derived from GIS-based thematic analysis. The agreement between surface-based groundwater potential mapping and geophysical observations demonstrates the effectiveness of combining remote sensing, GIS, and electrical resistivity methods for groundwater exploration.

Furthermore, validation using available well yield and lithological information increased the reliability of the final groundwater potential map (Arunbose et al., 2021; Genedi et al., 2025; Naiyeju et al., 2021). Such integrated approaches are particularly valuable in developing regions where groundwater exploration is challenging due to limited hydrogeological information and high exploration costs (Arunbose et al., 2021; Genedi et al., 2025; Naiyeju et al., 2021).

The groundwater potential map developed in this study provides an important scientific basis for groundwater exploration, water-resource planning, and sustainable management in Selamber District. The identified very good and excellent groundwater potential zones should be prioritized for future drilling and groundwater development because these areas represent favorable combinations of geological, structural, climatic, and hydrological conditions. However, groundwater potential mapping should be considered a regional-scale assessment tool, and detailed investigations such as exploratory drilling, pumping tests, and hydro-chemical analysis are recommended before large-scale groundwater development (Chandra, 2021; Khan et al., 2025; Kumar et al., 2022; Mohammed et al., 2025). Overall, the integrated GIS-AHP and VES methodology applied in this study provides an effective framework for reducing uncertainty in groundwater exploration and supports sustainable utilization of groundwater resources in water-stressed regions.

CONCLUSION AND RECOMMENDATION

Conclusion

This investigation reveals the integration of RS, GIS, and VES in delineating potential groundwater zones in the Selamber district, Southern Ethiopia. The seven thematic maps selected for the study were assigned weights and ranked using Saaty's Analytical Hierarchy Process, and the results were subjected to weighted overlay analysis. The resultant map was classified into five zones: very poor, poor, good, very good, and excellent, covering the area of 0.01, 15.71, 64.57, 19.28 and 0.43 % respectively.

The result of VES indicates varying hydrogeological conditions across the surveyed area. At all VES points, relatively low resistivity values have been identified at shallow depth. Thus, these are the sites where groundwater potential zones can be marked. The main water-bearing formations with good groundwater potential are alluvial sand and weathered basalt at about 50m

depth, and even at shallow depths in some areas. The apparent resistivity pseudo-sections also indicate that low resistivity values were encountered in the layer at shallow depth rather than in the layer at great depth below VES-4. Low resistivity layers also extend to greater depth; this indicates that the groundwater-bearing horizon extends to deep. The interpretation also suggests that geological structures may influence groundwater flow and occurrence.

Statements and Declarations

Competing interests: The authors declare that they have no competing interests.

Clinical trial declaration: not applicable.

Ethical approval: Not Applicable.
Consent to participate: Not Applicable.
Consent to publish: Not Applicable.
Competing interests: The authors declare no competing interests.
Funding: The Arba Minch University Research and Dissemination Office AMU/RDO/2022 funded this study.

Data availability: Data related to this paper will be made available upon reasonable request from the corresponding author.

Acknowledgments

The authors would like to express their gratitude to the Arba Minch University for their financial support of this study. And our gratitude extends Selamber people who encouraged us during field work.

Author Contributions Statement:

Tekle Bangu: Writing – original draft, Visualization, Methodology, Investigation, Data curation, Conceptualization, Writing – reviewing and editing. Arefegn Arota: Writing – original draft, Visualization, Methodology, Investigation, Data curation, Conceptualization, Writing – reviewing and editing. Teklehaimanot Teklearegay: Writing – original draft, Visualization,

Methodology, Investigation, Data curation, Conceptualization, Writing – reviewing and editing. Tariku Degife: Writing – original draft, Visualization, Methodology, Investigation, Data curation, Conceptualization, Writing – reviewing and editing. Muralitharan Jothimani- original draft, Visualization, Methodology, Investigation, Data curation, Conceptualization, Writing – reviewing and editing.

REFERENCES

Abijith, D., Saravanan, S., Singh, L., Jennifer, J.J., Saranya, T., Parthasarathy, K.S.S.,(2020). GIS-based multi-criteria analysis for identification of potential groundwater recharge zones - a case study from Ponnaniyaru watershed, Tamil Nadu, India. HydroResearch 3, 1–14. doi:10.1016/j.hydres.2020.02.002.

Agezew, T. (2015). Explanatory notes tohydrogeological and hydrochemical Maps of Jima NB 37 – 1 Sheet.

Alemayehu, T. (2006).Groundwater Occurrence in Ethiopia, Addis Ababa University, Addis Ababa, Ethiopia.

Amadi AN, Nwawulu CD, Unuevho CI, Okoye NO, Okunlola IA, Egharevba NA, Ako TA, Alkali YB (2011). Evaluation of the groundwater potential in Pompo Village, GidanKwano, Minna using Vertical Electrical Resistivity Sounding. Br J ApplSciTechnol 1: 53-66.

Anderson, E. I., & Bakker, M. (2008). Groundwater flow through anisotropic fault zones in multiaquifer systems. Water Resources Research, 44. https://doi.org/10.1029/2008wr006925

Annesh and Paresh (2015).High Resolution Groundwater Prospect Mapping of Raichur, Karnataka Using Remote Sensing and GIS.Imperial Journal of Interdisciplinary Research, 2(8).

Arunbose, S., Srinivas, Y., Rajkumar, S., Nair, N. C., & Kaliraj, S. (2021). Remote sensing, GIS and AHP techniques based investigation of groundwater potential zones in the Karumeniyar river basin, Tamil Nadu, southern India. Groundwater for Sustainable Development, 14, 100586. https://doi.org/10.1016/j.gsd.2021.100586

Ayalew, A., Tafesse, N. T., Hagos, M., & Matende, K. (2019). Characteristics and Productivity of Volcanic Rock Aquifers in the Upper Part of Blue Nile Basin, Ethiopia. Universal Journal of Geoscience. https://doi.org/10.13189/ujg.2019.070301

Ayenew T. and Abiye T. (2001).Principles of hydrogeology.Department of Earth Sciences, Addis Ababa Uuniveristy, Ethiopia.

Ayenew, T., Demlie, M., & Wohnlich, S. (2008). Hydrogeological framework and occurrence of groundwater in the Ethiopian aquifers. Journal of African Earth Sciences, 52, 97-113. https://doi.org/10.1016/j.jafrearsci.2008.06.006

Bera, A., Mukhopadhyay, B. P., & Das, D. (2019). Landslide hazard zonation mapping using multi-criteria analysis with the help of GIS techniques: a case study from Eastern Himalayas, Namchi, South Sikkim. *Natural Hazards, 962*(96), 935–959. https:// doi.org/ 10. 1007/ S11069- 019- 03580-W

Birhan, B., Mulshed, K., and Wondmneh, P. (2018). Explanatory notes to hydrogeological and hydrochemicalmapsofMaji (NB 36-8), Chido (NB 36-12) and Chido south (NB 36-16) map sheets.

Bretzler, A., Osenbrück, K., Gloaguen, R., Ruprecht, J. S., Kebede, S., & Stadler, S. (2011). Groundwater origin and flow dynamics in active rift systems – A multi-isotope approach in the Main Ethiopian Rift. Journal of Hydrology, 402, 274-289. https://doi.org/10.1016/j.jhydrol.2011.03.022

Chandra, P. (2021). Geophysics in Groundwater Exploration and Aquifer Mapping in India. Journal of the Geological Society of India, 97, 1106-1109. https://doi.org/10.1007/s12594-021-1827-7

Cid, H. E., Carrasco-Núñez, G., Manea, V., Vega, S., & Castaño, V. (2021). The role of microporosity on the permeability of volcanic-hosted geothermal reservoirs: A case study from Los Humeros, Mexico. Geothermics, 90, 102020. https://doi.org/10.1016/j.geothermics.2020.102020

Das, S. (2019). Comparison among influencing factor, frequency ratio, and analytical hierarchy process techniques for groundwater potential zonation in Vaitarna basin, Maharashtra, India.*Groundw. Sustain. Dev.*, *8*, 617–629, doi:10.1016/j.gsd.2019.03.003. 5. Todd, D.; Mays, L. *Groundwater Hydrology*; John Wiley & Sons: Hoboken, NJ, USA, 2004.

Das, S., & Pardeshi, S. D. (2018). Integration of different influencing factors in GIS to delineate groundwater potential areas using IF and FR techniques: a study of Pravara basin, Maharashtra, India. Applied Water Science, 8, 1-16. https://doi.org/10.1007/s13201-018-0848-x

Drury, S.A., (1987). Image Interpretation in Geology. (London: Allen &Unwin), 243pp.

Endyana, C., H., Sukiyah, E., & Dharmawan, I. A. (2016). Controlling Groudwater System by Pattern Fracture Approach in Subsurface Volcanic Deposit: Mt.Salak- Mt.Pangranggo, West Java, Indonesia. IOP Conference Series: Earth and Environmental Science, 29. https://doi.org/10.1088/1755-1315/29/1/012029

Fallatah, O., Ahmed, M., Cardace, D., Boving, T., & Akanda, A. (2019). Assessment of modern recharge to arid region aquifers using an integrated geophysical, geochemical, and remote sensing approach. Journal of Hydrology. https://doi.org/10.1016/j.jhydrol.2018.09.061

FAO (1985). Agro-climatological data for Africa: Food and agricultural organization of the United Nations, Rome, Italy.

Fenta, M. C., Anteneh, Z. L., Szanyi, J., & Walker, D. (2020). Hydrogeological framework of the volcanic aquifers and groundwater quality in Dangila Town and the surrounding area, Northwest Ethiopia. Groundwater for Sustainable Development. https://doi.org/10.1016/j.gsd.2020.100408

Gaikwad, S., Pawar, N.J., Bedse, P., Wagh, V. and Kadam, A. (2021).Delineation of groundwater potential zones using vertical electrical sounding (VES) in a complex bedrock geological setting of the West Coast of India. *Modeling Earth Systems and Environment*, pp.1-15.

Gastmans, D., Hutcheon, I., Menegário, A., & Chang, H. K. (2016). Geochemical evolution of groundwater in a basaltic aquifer based on chemical and stable isotopic data: case study from the Northeastern portion of Serra Geral Aquifer, São Paulo state (Brazil).. Journal of Hydrology, 535, 598-611. https://doi.org/10.1016/j.jhydrol.2016.02.016

Genedi, M. A., Gouhar, N., El-Qady, G., Gaafar, I., & Mahmoudi, A. E. (2025). Integrating conventional and remote sensing with DC resistivity datasets to map groundwater potential areas using the analytical hierarchy process method, North Wadi Diit, Egypt. Scientific Reports, 15. https://doi.org/10.1038/s41598-025-94598-7

Goitsemang, T., Das, D. M., Raul, S. K., Subudhi, C. R., &Panigrahi, B. (2020).Assessment of groundwater potential in the Kalahandi District of Odisha (India) using remote sensing, geographic information system and analytical hierarchy process.*Journal of theIndian Society of Remote Sensing, 48*, 1739–1753.https:// doi.org/10. 1007/ s12524- 020-01188-3

GSE (2014). Explanatory notes to hydrogeological and hydrochemical maps of Dila NB 37-6 sheet.

Gupta, D., Yadav, S., Tyagi, D., &Tomar, L. (2018). Multi-criteria decision analysis for identifying of groundwater potential sites in Haridwar, India. *The Engineering Journal of Application &Scopes, 3*, 9–15.

Hago, H. A. (2000). Application of Electrical Resistivity Methods in Quantitative Assessment of Groundwater Reserve of Unconfined Aquifer, University Putra Malaysia: 191 pp.

Halder, S., Roy, M. B., & Roy, P. K. (2020). Fuzzy logic algorithm based analytic hierarchy process for delineation of groundwater potential zones in complex topography. *Arabian Journal of Geosciences*.https:// doi.org/ 10. 1007/ s12517- 020- 05525-1.

Horton, R. E. (1945). Erosional development of streams and their drainage basins: Hydrophysical approach to quantitative morphology. *Geological Society of America Bulletin, 56*(3), 275–370. https://doi.org/10.1130/0016-7606(1945)56[275:EDOSAT]2.0.CO;2

Jana A, Biswas A, Arkoprovo B et al (2012) Delineation of groundwater potential zones using satellite remote sensing and geographic information system techniques: a case study from Ganjam district, Orissa, India. Res J Recent Sci 1:59–66

Jana A, Biswas A, Arkoprovo B et al (2012) Delineation ofgroundwater potential zones using satellite remote sensing andgeographic information system techniques: a case study fromGanjam district, Orissa, India. Res J Recent Sci 1:59–66

Jenks, G. F. (1967). The data model concept in statistical mapping. *International Yearbook of Cartography, 7*, 186–190.

Jerin, R., Pitchaimani, V., Kaliraj, S., Abishek, R., Antony, A., Promilton, A., & Karuppannan, S. (2025). Spatial modelling of groundwater potential zones in the Neyyar Basin using machine learning and morphometric analysis. Scientific Reports, 15. https://doi.org/10.1038/s41598-025-20000-1

Jothimani, M., Abebe, A., & Berhanu, G. (2022). Application of Remote Sensing, GIS, and Drainage Morphometric Analysis in Groundwater potential Assessment for sustainable development in Iyenda River Catchment, Konso Zone, Rift Valley, Southern Ethiopia. IOP Conference Series: Earth and Environmental Science, 982. https://doi.org/10.1088/1755-1315/982/1/012032

Kebede, S., Travi, Y., Asrat, A., Alemayehu, T., Ayenew, T., & Tessema, Z. (2008). Groundwater origin and flow along selected transects in Ethiopian rift volcanic aquifers. Hydrogeology Journal, 16, 55-73. https://doi.org/10.1007/s10040-007-0210-0.

Khan, L., Khan, S., Ali, M., Ali, M., & Kamal, M. (2025). Integrated Groundwater Potential and Quality Assessment in Pezu Dara Using Geophysical, GIS, and Hydrochemical Approaches. https://doi.org/10.22201/igeof.2954436xe.2026.65.1.1900

Khan, U., Faheem, H., Jiang, Z., Wajid, M., Younas, M., & Zhang, B. (2021). Integrating a GIS-Based Multi-Influence Factors Model with Hydro-Geophysical Exploration for Groundwater Potential and Hydrogeological Assessment: A Case Study in the Karak Watershed, Northern Pakistan. Water, 13, 1255. https://doi.org/10.3390/w13091255

Khanday, M. Y., & Javed, A. (2017). Hydrological investigations in the semi-arid Makhawan watershed, using morphometry. Applied Water Science, 7, 3919-3936. https://doi.org/10.1007/s13201-017-0545-1

Kowalsky, M.B., Gasperikova, E., Finsterle, S., Watson, D., Baker, G. and Hubbard, S.S. (2011).Coupled modeling of hydrogeochemical and andelectrical resistivity data for exploring the impact of recharge on subsurface contamination, Water Resources Research. Wiley Online Library, 47(2).

Krishnamurthy, J., Kumar, N.V., Jayaraman, V., and Manivel, M., (1996).An approach to demarcate groundwater potential zones through remote sensing and a geographic information system.Int. J. Remote Sensing, 17, pp. 1867-1885.

Krishnamurthy, J., Mani, A., Jayaraman, V., &Manivel, M. (2000). Groundwater resources development in hard rock terrain: An approach using remote sensing and GIS techniques. *InternationalJournal of Applied Earth Observation and Geoinformation, 2*, 204–215. https:// doi.org/ 10. 1016/ S0303- 2434(00) 85015-1

Kumar, C. P. (1997). Groundwater Assessment Methodology.National Institute of Hydrology, Roorkee 247667 (Uttaranchal).

Kumar, G., Kumar, D., & Warwade, P. (2022). GIS and geophysics: an integrative and inter-evaluating approach towards groundwater assessment. Geocarto International, 37, 15656 - 15682. https://doi.org/10.1080/10106049.2022.2102220

Lazarus, G. N and Yadav, G. S. (2014).Integration of Hydrogeological Factors for Identification of Groundwater Potential Zones Using Remote Sensing and GIS Techniques.GeosciencesandGeomatics, Vol. 2(1), Science and Education Publishing, p 11-16.

Lentswe, G. B., &Molwalefhe, L. (2020). Delineation of potential groundwater recharge zones using analytic hierarchy processguided GIS in the semi-arid Motloutse watershed, eastern Botswana. *Journal of Hydrology: Regional Studies, 28*, 100674.https:// doi.org/ 10. 1016/J. EJRH. 2020. 100674

Li, W., Macbean, N., Ciais, P., Defourny, P., Lamarche, C., Bontemps, S., Houghton, R. A., &Peng, S. (2018). Gross and net land cover changes in the main plant functional types derived from the annual ESA CCI land cover maps (1992–2015). *Earth System ScienceData, 10*, 219–234. https:// doi.org/ 10. 5194/ essd- 10- 219- 2018

Machiwal, D. M., Jha, K. B., Mal, C., Machiwal, D., Jha, M. K., & Mal, B. C. (2011). Assessment of groundwater potential in a semi-arid region of india using remote sensing, GIS and MCDM techniques. *Water Resource Management, 25*, 1359–1386. https:// doi.org/ 10.1007/ s11269- 010- 9749-y

Manap, M. A., Sulaiman, W. N. A., Ramli, M. F., Pradhan, B., &Surip, N. (2011). A knowledge-driven GIS modeling technique for groundwater potential mapping at the Upper Langat Basin, Malaysia.*Arabian Journal of Geosciences, 65*(6), 1621–1637. https:// doi.org/ 10. 1007/ S12517- 011- 0469-2

Mandal, U., Sahoo, S., Munusamy, S.B., Dhar, A., Panda, S.N., Kar, A., Mishra, P.K. (2016) Delineation of groundwater potential zones of coastal groundwater basin using multi-criteria decision making technique. Water Resourc.Managmt., v.30(12), pp.4293–4310. doi.org/10.1007/s11269- 016-1421-8

Mechal, A., Birk, S., Dietzel, M., Leis, A., Winkler, G., Mogessie, A., & Kebede, S. (2017). Groundwater flow dynamics in the complex aquifer system of Gidabo River Basin (Ethiopian Rift): a multi-proxy approach. Hydrogeology Journal, 25, 519-538. https://doi.org/10.1007/s10040-016-1489-5

Mihret, B., & Wuletaw, A. (2025). The impact of geological structures on groundwater potential assessment in volcanic rocks in the Borena Sayint district, northwestern Ethiopian Plateau: a review. Hydrology and Earth System Sciences. https://doi.org/10.5194/hess-29-2951-2025

Ministry of Water, Irrigation and Energy (MoWIE).(2007). Overview of Ethiopia's groundwater resources. Addis Ababa, Ethiopia.

Moeck, C., Grech-Cumbo, N., Podgorski, J., Bretzler, A., Gurdak, J., Berg, M., & Schirmer, M. (2020). A global-scale dataset of direct natural groundwater recharge rates: A review of variables, processes and relationships.. The Science of the total environment, 717, 137042 . https://doi.org/10.1016/j.scitotenv.2020.137042

Mohammed, S., Mohammed, M. A. A., Karim, H., Al-Manmi, D., Aziz, B. Q., Mustafa, A. I., & Szűcs, P. (2025). Integrating geospatial, hydrogeological, and geophysical data to identify groundwater recharge potential zones in the Sulaymaniyah basin, NE of Iraq. Scientific Reports, 15. https://doi.org/10.1038/s41598-025-94603-z

Mohammed, S., Mohammed, M. A. A., Karim, H., Al-Manmi, D., Aziz, B. Q., Mustafa, A. I., & Szűcs, P. (2025). Integrating geospatial, hydrogeological, and geophysical data to identify groundwater recharge potential zones in the Sulaymaniyah basin, NE of Iraq. Scientific Reports, 15. https://doi.org/10.1038/s41598-025-94603-z

Mohan, C., Western, A., Wei, Y., & Saft, M. (2017). Predicting groundwater recharge for varying land cover and climate conditions – a global meta-study. Hydrology and Earth System Sciences, 22, 2689-2703. https://doi.org/10.5194/hess-22-2689-2018

Morris, B., Lawrence, A.R.L., Chilton, P.J.C., Adams, B., Calow, R.C. (2003). Groundwater and its Susceptibility to Degradation.A Global Assessment of the Problem and Options for Management.

Naiyeju, J. O., Oladunjoye, M., & Adeniran, M. A. (2021). Aquifer evaluation in parts of north-central Nigeria from geo-electrical derived parameters. Applied Water Science, 11. https://doi.org/10.1007/s13201-021-01520-3

Ndatuwong LG, Yadav GS (2015).Application of geo-electrical data to evaluate groundwater potential zone and assessment of overburden protective capacity in part of Sonebhadra district, Uttar Pradesh. Environ Earth Sci 73:3655–3664. Doi: 10.1007/s12665-014-3649-z.

Ortenzi, S., Di Matteo, L., Valigi, D., Donnini, M., Dionigi, M., Fronzi, D., Geris, J., Guadagnano, F., Marchesini, I., Filippucci, P., Avanzi, F., Penna, D., & Massari, C. (2026). Exploring groundwater-surface water interactions and recharge in fractured mountain systems: an integrated approach. Hydrology and Earth System Sciences. https://doi.org/10.5194/hess-30-1755-2026

Oyda, Y., Hatiye, S.D. & Jothimani, M. Identification of groundwater potential zones using geospatial analysis and frequency ratio model: the case of Kulfo-Hamassa watershed, Rift Valley, Ethiopia. Discov Appl Sci 7, 571 (2025). https://doi.org/10.1007/s42452-025-07092-0

Patil, S. G., &Mohite, N. M. (2014). Identification of groundwater recharge potential zones for a watershed using remote sensing and GIS. *International Journal of Geomatics and Geosciences,4*, 485–498.

Patil, V.B., Lokesh, K.N., Krishnamurthy, M.P. and Nadagoudar, H.V. (2020). Delineation of groundwater potential zones using integrated approach in semi-arid hard rock terrain, KanaviHalla Sub-Basin, Belagavi District, Karnataka. *Journal of the Geological Society of India*, *96*(4), pp.410-419.

Prasad, R., K., Mondal, N. C., Banerjee, P., Nandakumar, M. V., and Singh, V. S., (2008).Deciphering potential groundwater zone in hard rock through the application of GIS.Environmental geology, 467-475.

Rajaveni, S. P., Brindha, K., & Elango, L. (2017). Geological and geomorphological controls on groundwater occurrence in a hard rock region. Applied Water Science, 7, 1377-1389. https://doi.org/10.1007/s13201-015-0327-6

Sahoo, S., Munusamy, S. B., Dhar, A., Kar, A., & Ram, P. (2017).Appraising the accuracy of multi-class frequency ratio and weights of evidence method for delineation of regional groundwater potential zones in canal command system.*Water ResourceManagement, 3114*(31), 4399–4413. https:// doi.org/ 10. 1007/S11269- 017- 1754-Y

Sapkota, A., Lamsal, S., & Paudyal, K. (2024). Mountain hydrogeology and influence of active fault: A study of the Bhimgethi-Devisthan section in Western Nepal. Journal of Nepal Hydrogeological Association. https://doi.org/10.3126/jnha.v1i1.78218

Seenipandi, K., Nainarpandian, C., Kandathil, R. K., &Sellamuthu, S. (2019). Seawater intrusion vulnerability in the coastal aquifers of southern India: An appraisal of the GALDIT

model, parameters' sensitivity, and hydrochemical indicators. *Environmental Scienceand Pollution Research, 26*, 9755–9784. https:// doi.org/ 10. 1007/S11356- 019- 04401-0

Shaban, A., Khawlie, M., Abdallah, C., (2006). Use of remote sensing and GIS to determine recharge potential zones: the case of Occidental Lebanon. Hydrogeology Journal 14 (4), 433e443.

Shao, Z., Huq, M. E., Cai, B., Altan, O., & Li, Y. (2020). Integrated remote sensing and GIS approach using Fuzzy-AHP to delineate and identify groundwater potential zones in semi-arid Shanxi Province, China. *Environmental Modelling& Software, 134*, 104868.https:// doi.org/ 10. 1016/J. ENVSO FT. 2020. 104868

Siva, G., Nasir, N., &Selvakumar, R. (2017).Delineation of groundwater potential zone in sengipatti for Thanjavur District using analytical hierarchy process.*IOP Conference Series: Earth andEnvironmental Science, 80*, 012063. https:// doi.org/ 10. 1088/ 1755-1315/ 80/1/ 012063

Tesfaye, T. (2012). Ground water potential evaluation based on integrated GIS and remote sensing techniques, in bilate river catchment: south rift valley of Ethiopia (AAU).

Thapa, R., Gupta, S., Guin, S., &Kaur, H. (2017). Assessment of groundwater potential zones using multi-influencing factor (MIF) and GIS: A case study from Birbhum district, West Bengal. *Applied Water Science, 7*, 4117–4131.https:// doi.org/ 10. 1007/S13201- 017 0571-Z

Tolba, A.A., Hatiye, S.D. & Jothimani, M. Identification of groundwater potential zones in drought prone Bazo River catchment, Southern Ethiopia using GIS, AHP and FR techniques. Discov Appl Sci 8, 738 (2026). https://doi.org/10.1007/s42452-026-08775-y

Varade, A. M., Khare, Y. D., Yadav, P., Doad, A. P., Das, S., Kanetkar, M., &Golekar, R. B. (2018). 'Lineaments' the potential groundwater zones in hard rock area: A case study of Basaltic Terrain of WGKKC-2 Watershed from Kalmeswar Tehsil of Nagpur District, Central India. *Journal of the Indian Society of Remote Sensing, 46*,539–549.https:// doi.org/ 10. 1007/ S12524- 017- 0716-4

Yeh, H.-F.; Lee, C.-H.; Hsu, K.-C.; Chang, P.-H. (2008). GIS for the assessment of the groundwater recharge potential zone. Environ. Earth Sci. 58, 185–195.

Zaidi FK, Kassem OMK (2012). Use of electrical resistivity tomography in delineating zones of groundwater potential in arid regions: a case study from Diriyah region of Saudi Arabia. Arab J Geosci 5:327–333. Doi: 10.1007/s12517-010-0165-7.

APPENDICES:

Appendix-1:

Factor	Classes	Area in (Km^2)	Area in (%)	Groundwater prospect	CI	RI	CR
Lithology	Basalt	410.37	64.6	Very good	0	0.52	0
	Volcanic tuff	167.8	26.42	Good			
	Ignimbrite	57.03	8.98	Moderately good			
Lineament density	0.00-0.019	255.72	40	Very low	0.03	1.12	0.02
	0.020-0.053	128.82	20	Low			
	0.054-0.081	173.47	27	Low to moderate			
	0.082-0.110	51.27	8	Moderate			
	0.120-0.180	25.72	4	High			
Rainfall	297-477	82	13	Very low	0.03	0.03	0.03
	478-624	104.9	17	Low			
	625-756	171.6	27	Low to moderate			
	757-890	139.46	22	Moderate			
	891-1154	137.04	22	High			
Slope	0-7	212.68	33	High	-0.002	1.12	-0.001
	7.1-14	183.91	29	Moderate			
	15-21	118.65	19	Low to moderate			
	22-31	81.96	13	Low			
	32-64	37.8	6	Very low			
Drainage density	0.00-0.83	278.61	44	High	-0.003	0.90	-0.003
	0.83-1.00	172.83	27	Moderate			
	1.00-1.19	128	20	Low			
	1.19-1.58	55.56	9	Very low			
LULC	Built up area	132	20.70	Very poor			
	Barren land	101	16	Poor			

	Cultivated land	210	33.07	Moderately good	0.03	1.12	0.02
	Vegetation	182	28.66	Good			
	Water body	10	1.57	Very good			
Soil	Dystricfluvisols	51.37	8.10	High	-0.003	0.9	-0.003
	EutricCambisols	43.85	49.76	Moderate			
	OrthicAcrisols	223.80	6.90	Low			
	Dystricnitisols	316	35.24	Very low			

Appendix-2: Long term temperature of the study area in Dana station located at longitude 037^0 34' 15.6" E, latitude 06^0 38' 07.2" N and altitude = 1279m

Year	Jan	Feb	Mar	Apr	May	Jun	Jul	Aug	Sep	Oct	Nov	Dec
2009	32.00	32.26	32.90	31.56	30.42	27.10	31.19	30.08	31.07	30.86	32.14	31.20
2010	27.41	30.63	30.95	29.00	27.56	28.28	27.56	28.90	27.71	29.96	30.17	28.85
2011	29.98	30.89	30.64	28.95	26.90	26.52	27.25	27.90	27.18	28.04	27.98	27.90
2012	30.26	32.44	33.60	28.55	29.70	25.30	26.76	26.71	27.28	29.41	30.10	29.60
2013	33.35	30.78	31.59	28.13	28.97	27.20	27.25	27.90	27.30	29.57	29.00	30.20
2014	31.48	31.96	32.83	32.18	30.60	30.17	29.68	29.00	29.07	29.37	28.00	32.92
2015	32.39	33.73	33.80	32.00	32.20	30.45	30.56	30.90	30.70	31.24	31.08	31.90
2016	33.03	33.67	34.61	32.10	29.90	30.10	30.29	27.80	31.13	30.42	30.50	33.60
2017	29.30	29.80	33.64	33.13	31.90	31.40	28.48	29.45	28.93	31.06	31.57	30.82
2018	31.94	32.40	32.75	34.20	32.00	29.40	27.87	28.00	ND	31.26	30.06	29.63
Av.max.T (˚C)	31.11	31.86	32.73	30.98	30.01	28.59	28.69	28.66	28.93	30.12	30.06	30.66
2009	14.90	17.20	17.56	16.31	17.40	17.38	14.51	14.00	16.88	16.49	14.48	15.95
2010	16.13	17.74	16.00	15.96	18.90	17.89	16.72	16.37	17.03	16.00	15.30	16.06
2011	14.98	15.70	19.00	17.55	12.23	15.43	15.00	12.00	13.90	12.92	12.62	15.80
2012	15.90	17.00	15.00	18.84	13.30	12.58	14.00	13.86	15.00	13.60	18.10	17.00
2013	16.00	13.96	18.79	15.00	16.00	15.00	13.00	15.00	17.00	15.00	15.61	ND
2014	16.00	13.89	17.00	16.85	17.00	13.00	11.03	15.90	14.15	16.51	16.00	ND
2015	15.20	18.00	16.00	13.09	14.00	17.17	13.48	14.00	15.00	15.72	15.20	16.31
2016	16.49	16.29	18.00	18.00	15.59	16.85	21.71	15.50	16.90	15.70	14.45	15.04
2017	13.90	14.10	15.00	16.00	13.12	15.75	16.90	16.00	ND	15.20	15.60	ND
2018	14.70	15.64	18.00	13.00	15.55	ND	16.00	14.94	ND	17.81	ND	ND
Av.min.T.(˚C)	15.42	15.95	17.04	16.06	15.31	15.67	15.24	14.76	15.73	15.49	15.26	16.03